Advanced techniques in scientific computing. Application to electromagnetics

Adrián Amor-Martín

Advisor: Luis E. García-Castillo

December 5, 2018

University Carlos III of Madrid

Introduction

Antecedents:

- 20 years on numerical methods (FEM) for EM.
    - Mixed-order curl-conforming basis functions.
    - Non-standard mesh truncation technique.
    - Adaptivity: *h* and *hp*.
    - Hybridization with MoM, PO/PTD and GTD/UTD.

GREMA
RADIOFREQUENCY, ELECTROMAGNETICS, MICROWAVES & ANTENNAS

In-house electromagnetic suite, HOFEM:

- User-friendly (based on GiD).

FEM

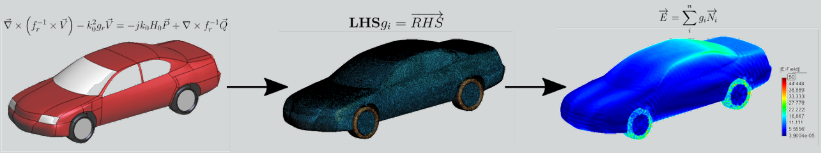

D. García-Doñoro, "A new software suite for electromagnetics", advisors: L.E. García-Castillo, T.K. Sarkar; University Carlos III of Madrid, 2014.

In-house electromagnetic suite, HOFEM:

- User-friendly (based on GiD).
- Efficient use of HPC in electromagnetics.

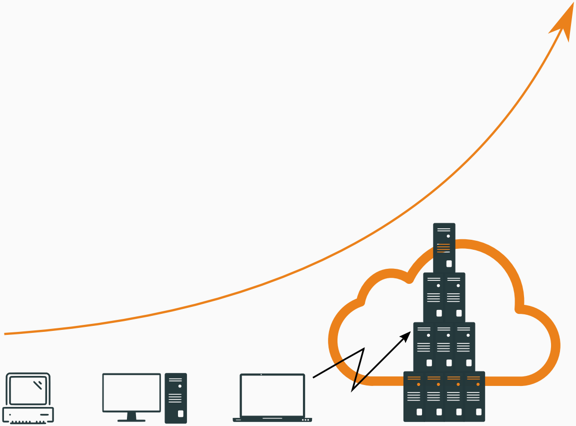

GREMA
RADIOFREQUENCY, ELECTROMAGNETICS, MICROWAVES & ANTENNAS

In-house electromagnetic suite, HOFEM:

- Efficient use of HPC in electromagnetics.

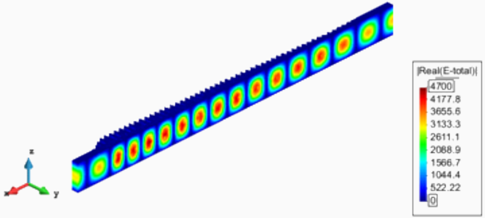

70M unknowns, 1000 cores, Tianhe-2 supercomputer (Guangzhou, China).

D. García-Doñoro, **A. Amor-Martín**, and L. E. García-Castillo, ”Higher-Order Finite Element Electromagnetics Code for HPC Environments,” *Procedia Computer Science*, vol. 108, pp. 818-827, 2017.

Applications:

Waveguides

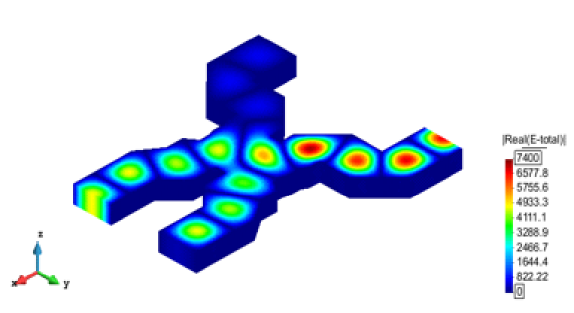

D. García-Doñoro, "A new software suite for electromagnetics", advisors: L.E. García-Castillo, T.K. Sarkar; University Carlos III of Madrid, 2014.

Applications:

Antennas

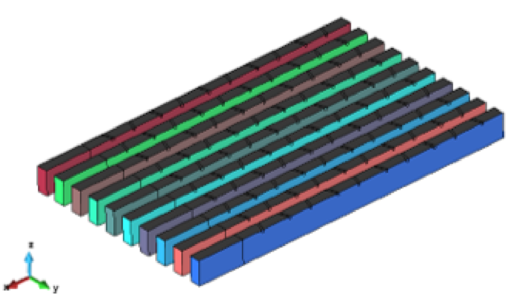

D. García-Doñoro, ”A new software suite for electromagnetics”, advisors: L.E. García-Castillo, T.K. Sarkar; University Carlos III of Madrid, 2014.

Applications:

Antennas

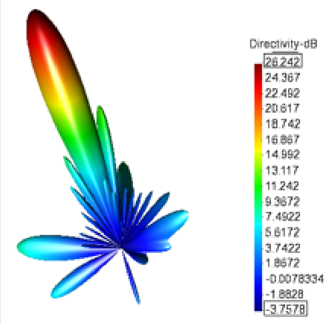

D. García-Doñoro, "A new software suite for electromagnetics", advisors: L.E. García-Castillo, T.K. Sarkar; University Carlos III of Madrid, 2014.

Applications:

RCS

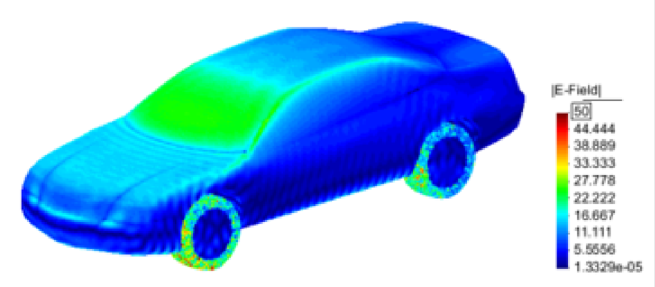

D. García-Doñoro, "A new software suite for electromagnetics", advisors: L.E. García-Castillo, T.K. Sarkar; University Carlos III of Madrid, 2014.

Applications:

SAR

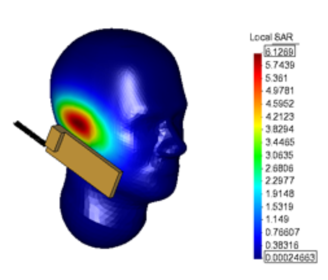

D. García-Doñoro, ”A new software suite for electromagnetics”, advisors: L.E. García-Castillo, T.K. Sarkar; University Carlos III of Madrid, 2014.

Room for improvement:

- More shapes.
- Support for *hp* meshes.
    - Automatic *h* adaptivity.
    - Basis functions for *p* adaptivity.
- Iterative solvers.

Some considerations about adaptivity:

- *h* refinement.

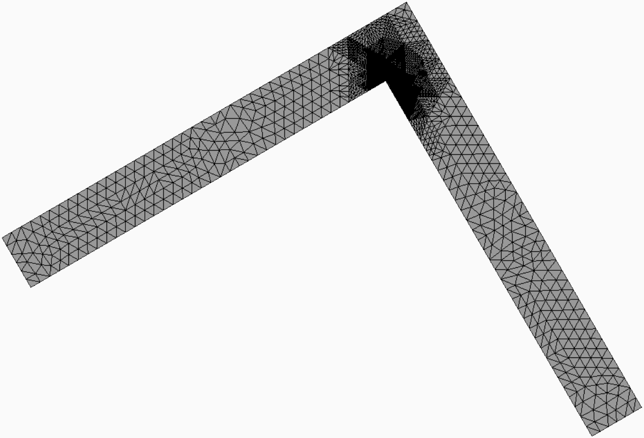

Some considerations about adaptivity:

- h refinement.
- p refinement.

Some considerations about adaptivity:

- h refinement.
- p refinement.
- Exponential error convergence with hp adaptivity.
  - Coarse-fine grid prohibitive in 3D EM engineering.
  - Division into subdomains $\Rightarrow$ lack of independence.

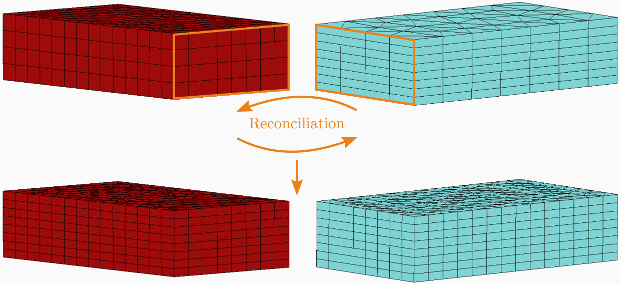

GREMA RADIOFREQUENCY, ELECTROMAGNETICS, MICROWAVES & ANTENNAS

Viability of a non-conformal domain decomposition method (DDM) supporting parallel scalable hp adaptivity

Viability of a non-conformal domain decomposition method (DDM) supporting parallel scalable hp adaptivity

Viability of a non-conformal domain decomposition method (DDM) supporting parallel scalable hp adaptivity

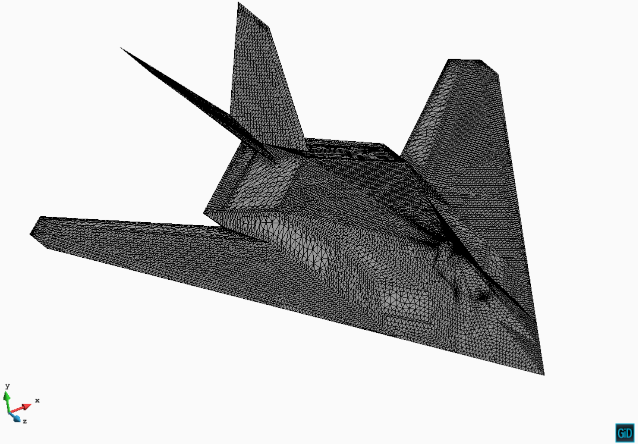
y
x
z

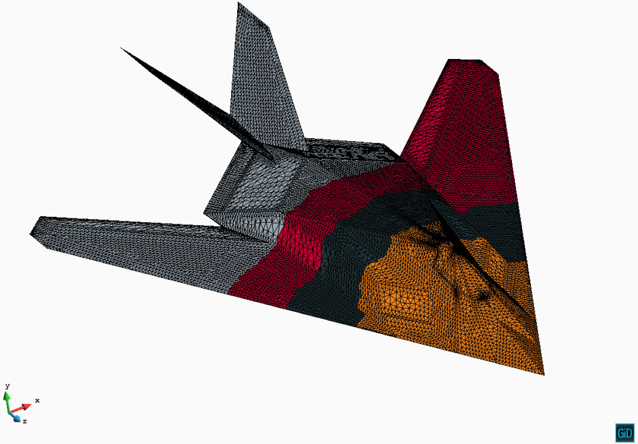
y
x
z
GiD

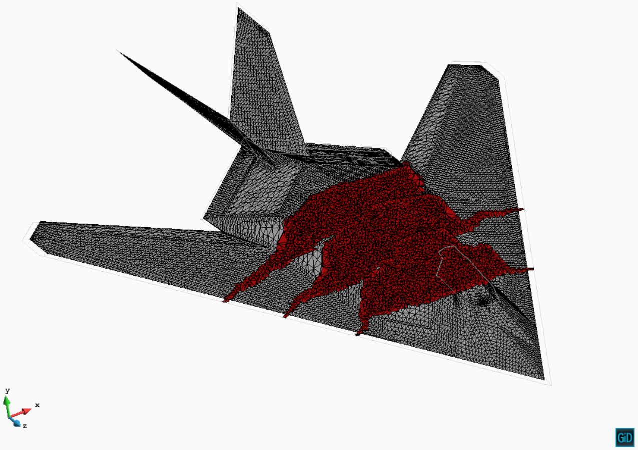
y
x
z
GiD

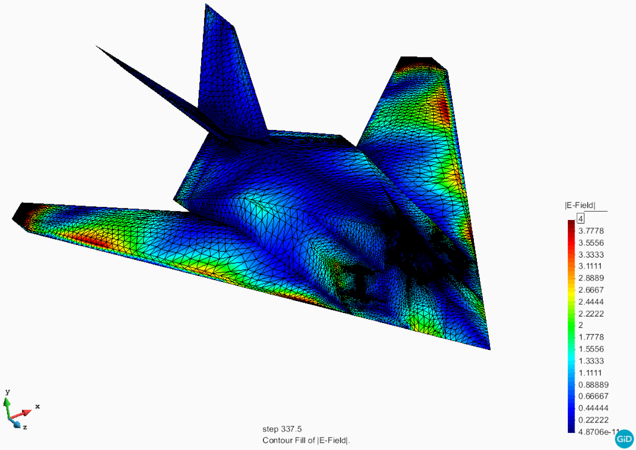
|E-Field|
4
3.7778
3.5556
3.3333
3.1111
2.8889
2.6667
2.4444
2.2222
2
1.7778
1.5556
1.3333
1.1111
0.88889
0.66667
0.44444
0.22222
4.8706e-11
GiD
y
x
z
step 337.5
Contour Fill of |E-Field|.

Classification:

- Solution of the surface problem.

GREMA
RADIOFREQUENCY, ELECTROMAGNETICS, MICROWAVES & ANTENNAS

Classification:

- Solution of the surface problem.
- Overlapping vs non-overlapping.

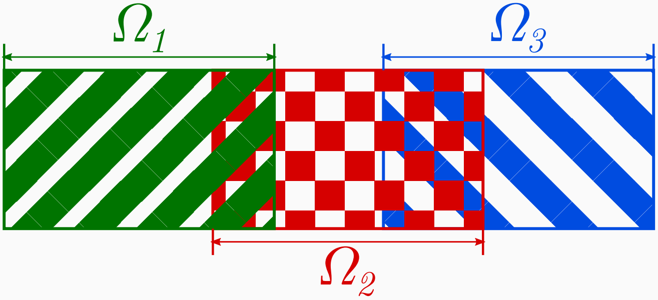

Classification:

- Solution of the surface problem.
- Overlapping vs non-overlapping.
- Conformal vs non-conformal.

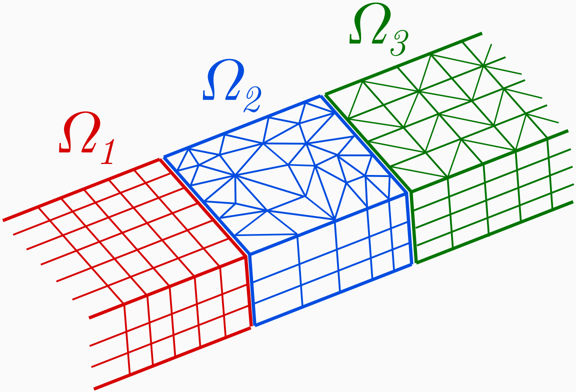

Main advantages of DDM:

- Suitable for large problems.
- Parallelization.
- Preconditioner for iterative solvers.

GREMA
RADIOFREQUENCY, ELECTROMAGNETICS, MICROWAVES & ANTENNAS

Additional advantages from non-conformal DDM:

- Independent meshes.
- Non-conformal meshes in periodic structures.
- Full parallel adaptivity.
- Different FEM shapes/families for each subdomain.

Intro: contributions

Main contributions:

- Basis functions.
- Non-conformal and non-overlapping DDM.
- Adaptivity with NCDDM.

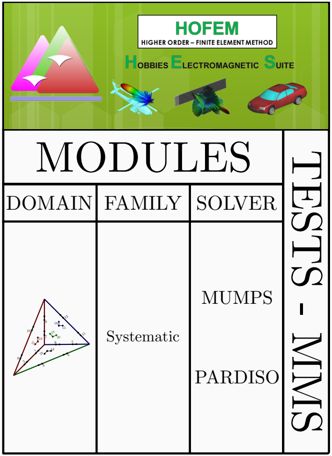

Intro: contributions

Main contributions:

- Basis functions.
  - New shapes: prisms and hexahedra.
  - New FEM family for *p* refinement.
- Non-conformal and non-overlapping DDM.
- Adaptivity with NCDDM.

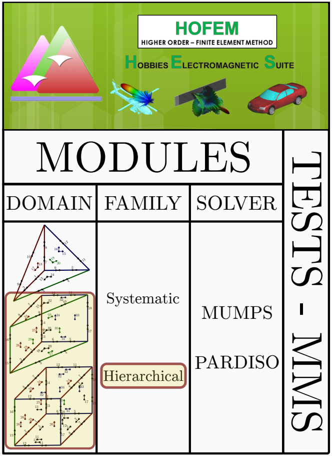

Main contributions:

- Basis functions.
- Non-conformal and non-overlapping DDM.
  - Verification and validation.
  - Three-level parallelization.
  - Study of non-conformality accuracy.
- Adaptivity with NCDDM.

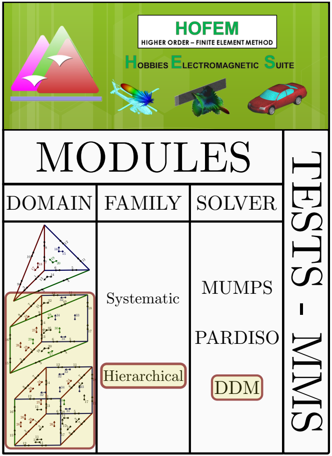

Main contributions:

- Basis functions.
- Non-conformal and non-overlapping DDM.
- Adaptivity with NCDDM.
    - Using triangular prisms.
    - Influence of NCDDM.

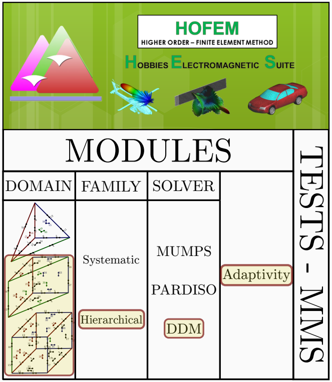

Table of contents

Basis functions

GREMA
RADIOFREQUENCY, ELECTROMAGNETICS, MICROWAVES & ANTENNAS

Chronology:

- Nedelec:
  - Curl-conforming.
  - Mixed-order.
- Classification:
  - Interpolatory basis functions.
  - Hierarchical basis functions.
- Jin-Fa Lee and Csendes (1991), Webb (1993), Graglia et al. (1997), García-Castillo and Salazar-Palma (1998), Ilic and Notaros (2003).

Two FEM families introduced:

- Own development.
- Hierarchical family.

Basis functions

Systematic approach

Basic concepts:

- FEM: domain, space of functions and DOFs.
- Obtained with a systematic approach:
  - Known space of functions.
  - *A priori* definition of DOFs as functionals.
  - Basis functions as dual basis with respect to those DOFs.
- Mixed-order family: tetrahedron, 1998, triangular prism, 2016, hexahedron, 201?.

GREMA
RADIOFREQUENCY, ELECTROMAGNETICS, MICROWAVES & ANTENNAS

- Tetrahedra,
$$\boldsymbol{\mathcal{R}}_{\boldsymbol{k}} = \left\{ \mathbf{u} \in \mathbf{P}_k ; \epsilon^k(\mathbf{u}) = 0 \right\}.$$
- Triangular prism: tensor product between triangle and segment,
$$\boldsymbol{\mathcal{P}}_{\boldsymbol{k}}^{\text{prism}} = \left(\boldsymbol{\mathcal{R}}_{\boldsymbol{k}}(T) \otimes P_k(I) \right) \times \left(\mathbf{P}_k(T) \otimes P_{k-1}(I) \right).$$
- Hexahedra: tensor product between segments in 3D,
$$\begin{aligned} \boldsymbol{\mathcal{P}}_{\boldsymbol{k}}^{\text{hexa}} = & \left(P_{k-1}(I) \otimes P_k(I) \otimes P_k(I) \right) \\ & \times \left(P_k(I) \otimes P_{k-1}(I) \otimes P_k(I) \right) \\ & \times \left(P_k(I) \otimes P_k(I) \otimes P_{k-1}(I) \right). \end{aligned}$$

Coefficients for the second-order triangular prism:

$$\mathbf{N}_i = \left\{ \begin{array}{c} a_1^{(i)} + a_2^{(i)}\xi + a_3^{(i)}\eta + a_4^{(i)}\zeta + a_5^{(i)}\xi\zeta + a_6^{(i)}\eta\zeta + a_7^{(i)}\zeta^2 + a_8^{(i)}\xi\zeta^2 + \ldots \\ \ldots + a_9^{(i)}\eta\zeta^2 + C^{(i)}\eta^2 + D^{(i)}\xi\eta + E^{(i)}\eta^2\zeta + F^{(i)}\xi\eta\zeta + G^{(i)}\eta^2\zeta^2 + H^{(i)}\xi\eta\zeta^2 \\ \\ b_1^{(i)} + b_2^{(i)}\xi + b_3^{(i)}\eta + b_4^{(i)}\zeta + b_5^{(i)}\xi\zeta + b_6^{(i)}\eta\zeta + b_7^{(i)}\zeta^2 + b_8^{(i)}\xi\zeta^2 + \ldots \\ \ldots + b_9^{(i)}\eta\zeta^2 - C^{(i)}\xi\eta - D^{(i)}\xi^2 - E^{(i)}\xi\eta\zeta - F^{(i)}\xi^2\zeta - G^{(i)}\xi\eta\zeta^2 - H^{(i)}\xi^2\zeta^2 \\ \\ c_1^{(i)} + c_2^{(i)}\xi + c_3^{(i)}\eta + c_4^{(i)}\xi^2 + c_5^{(i)}\eta^2 + c_6^{(i)}\xi\eta + c_7^{(i)}\zeta + c_8^{(i)}\xi\zeta + \ldots \\ \ldots + c_9^{(i)}\eta\zeta + c_{10}^{(i)}\xi^2\zeta + c_{11}^{(i)}\eta^2\zeta + c_{12}^{(i)}\xi\eta\zeta \end{array} \right\}$$

Degrees of Freedom:

- Edges,
$$g(\mathbf{u}) = \int_e (\mathbf{u} \cdot \hat{\boldsymbol{\tau}})\, q \, dl, \forall q \in P_1(e).$$
- Triangular faces,
$$g(\mathbf{u}) = \int_{f_t} (\mathbf{u} \times \widehat{\mathbf{n}}) \cdot \mathbf{q} \, ds, \forall \mathbf{q} \in \mathbf{P}_0(f_t).$$
- Quadrilateral faces,
$$g(\mathbf{u}) = \int_{f_q} (\widehat{\mathbf{n}} \times \mathbf{u}) \cdot \mathbf{q} \, ds, \forall \mathbf{q} = (q_1, q_2); q_1 \in \mathcal{Q}_{0,1}; q_2 \in \mathcal{Q}_{1,0}.$$
- Volume,
$$g(\mathbf{u}) = \int_v \mathbf{u} \cdot \mathbf{q} \, dV, \forall \mathbf{q} \in \mathbf{P}_0.$$

GREMA
RADIOFREQUENCY, ELECTROMAGNETICS, MICROWAVES & ANTENNAS

Dual basis:

$$g_i(\mathbf{N_j}) = \delta_{ij}$$

$$\begin{cases} a_1^{(i)} g_i([1,0,0]) + \ldots + D^{(i)} g_i([\xi\eta, \xi^2, 0]) + \ldots + c_{12}^{(i)} g_i([0,0,\xi\eta\zeta]) = 1 \\ a_1^{(j)} g_i([1,0,0]) + a_2^{(j)} g_i([\xi,0,0])0 + \ldots + c_{12}^{(j)} g_i([0,0,\xi\eta\zeta]) = 0 \\ a_1^{(i)} g_j([1,0,0]) + \ldots + b_4^{(i)}([0,\zeta,0]) + \ldots + c_{12}^{(i)} g_j([0,0,\xi\eta\zeta]) = 0 \end{cases}$$

- Discretization: choice of $q, \mathbf{q}$.
- Local definition of $\hat{\boldsymbol{\tau}}$, $\widehat{\mathbf{n}}$ and directions of $\mathbf{q}$.
- Use of a master element,

$$\mathbf{u} = [J]^{-1}\widehat{\mathbf{u}}.$$

Basis functions: master element

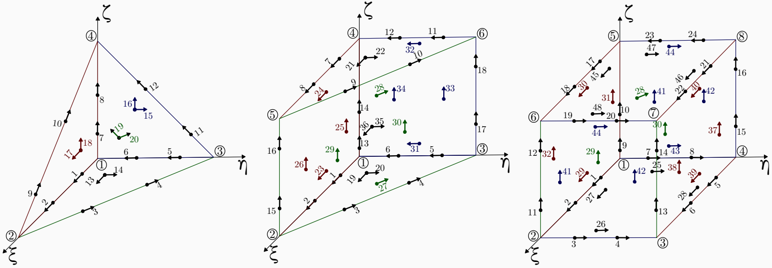

Kernel formulation for verification:

$$\nabla \times \frac{1}{\mu_r}(\nabla \times \mathbf{E}) - k_0^2 \varepsilon_r \mathbf{E} = \mathbf{O}$$

$$\widehat{\mathbf{n}} \times \mathbf{E} = \mathbf{d}, \text{ on } \Gamma_D;\ \mathbf{d} = 0 \text{ with PEC}$$

$$\widehat{\mathbf{n}} \times \frac{1}{\mu_r}(\nabla \times \mathbf{E}) = \mathbf{b}, \text{ on } \Gamma_N;\ \mathbf{b} = 0 \text{ with PMC}$$

$$\widehat{\mathbf{n}} \times \frac{1}{\mu_r}(\nabla \times \mathbf{E}) + jk_0 \widehat{\mathbf{n}} \times \widehat{\mathbf{n}} \times \mathbf{E} = \mathbf{c}, \text{on } \Gamma_C$$

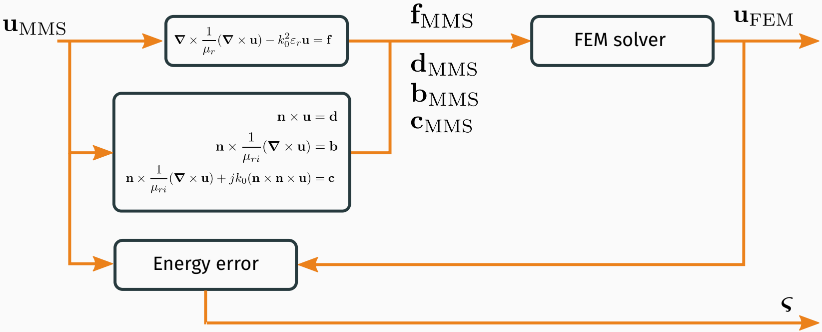

Garcia-Doñoro, D., Garcia-Castillo, L. E., and Ting, S. W. (2016). Verification Process of Finite-Element Method Code for Electromagnetics. IEEE Antennas and Propagation Magazine, 1045(9243/16).

GREMA RADIOFREQUENCY, ELECTROMAGNETICS, MICROWAVES & ANTENNAS

Monomials:

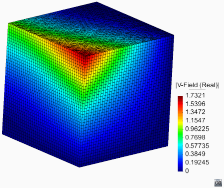

$|\mathbf{u}_{\text{MMS}}|$

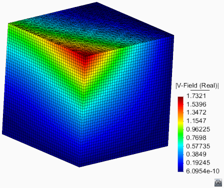

$|\mathbf{u}_{\text{FEM}}|$

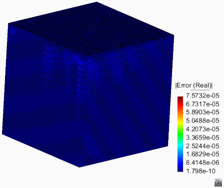

ς_p

$$(xyz^2, -xz^2, xyz)$$

$$\varsigma_p = |\mathbf{u}_{\text{MMS}} - \mathbf{u}_{\text{FEM}}|$$

Smooth functions:

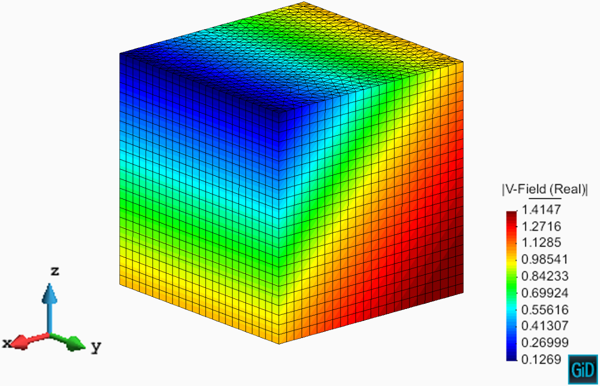

A. Amor-Martín, L. E. García-Castillo, and D. García-Doñoro, ”Second-Order Nédélec Curl-Conforming Prismatic Element for Computational Electromagnetics,” *IEEE Transactions on Antennas and Propagation*, vol. 64, no. 10, pp. 4384-4395, 2016.

Smooth functions:

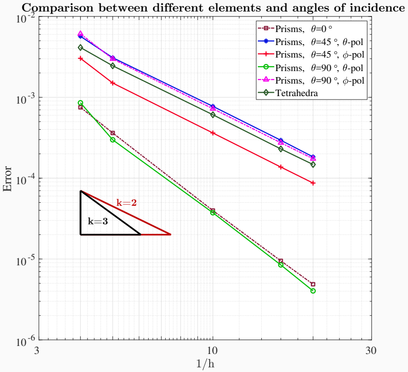

A. Amor-Martín, L. E. García-Castillo, and D. García-Doñoro, ”Second-Order Nédélec Curl-Conforming Prismatic Element for Computational Electromagnetics,” *IEEE Transactions on Antennas and Propagation*, vol. 64, no. 10, pp. 4384-4395, 2016.

DGS band-pass filter:

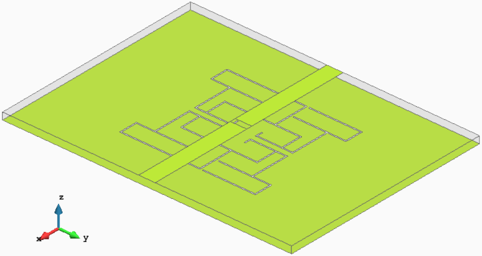

D. García-Doñoro, S. Ting, **A. Amor-Martín**, and L. E. García-Castillo, "Analysis of Planar Microwave Devices using Higher Order Curl-Conforming Triangular Prismatic Finite Elements," *Microwave and Optical Technology Letters*, vol. 58, no. 8, pp. 1794-1801, 2016.

DGS band-pass filter:

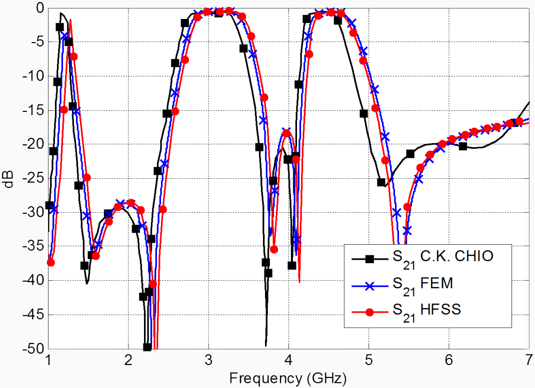

D. García-Doñoro, S. Ting, **A. Amor-Martín**, and L. E. García-Castillo, "Analysis of Planar Microwave Devices using Higher Order Curl-Conforming Triangular Prismatic Finite Elements," *Microwave and Optical Technology Letters*, vol. 58, no. 8, pp. 1794-1801, 2016.

Basis functions

Hierarchical family

GREMA
RADIOFREQUENCY, ELECTROMAGNETICS, MICROWAVES & ANTENNAS

- Hierarchical vector basis functions.
- Four classical energy spaces: H^1, H(curl), H(div) and L^2.
- Ready for p-refinement.

F. Fuentes, B. Keith, L. Demkowicz, S. Nagaraj, “Orientation embedded high order shape functions for the exact sequence elements of all shapes”, *Computers & Mathematics with Applications*, 70:353–458, 2015.

Basis functions: MMS with *p* ref.

GREMA
RADIOFREQUENCY, ELECTROMAGNETICS, MICROWAVES & ANTENNAS

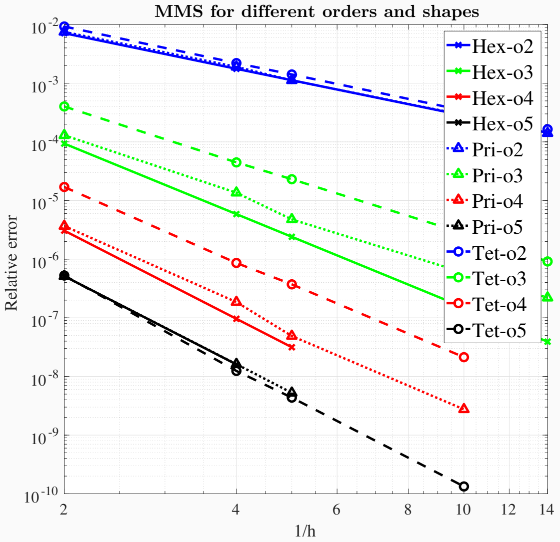

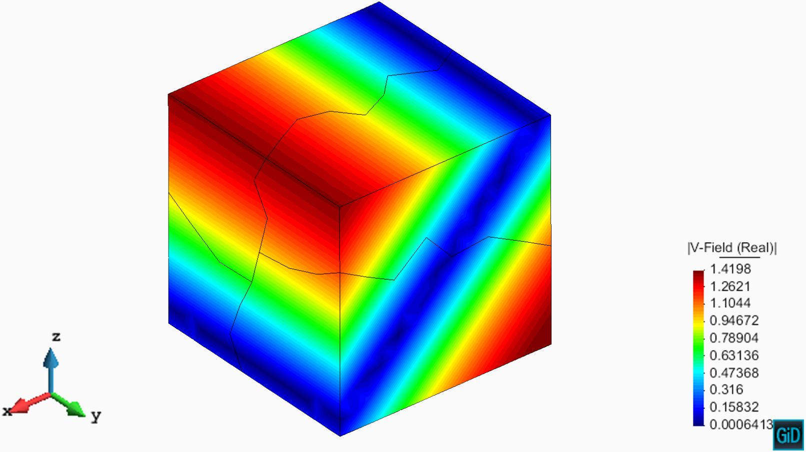

$|\mathbf{u}_{\mathrm{MMS}}|$

Basis functions: MMS with p variable

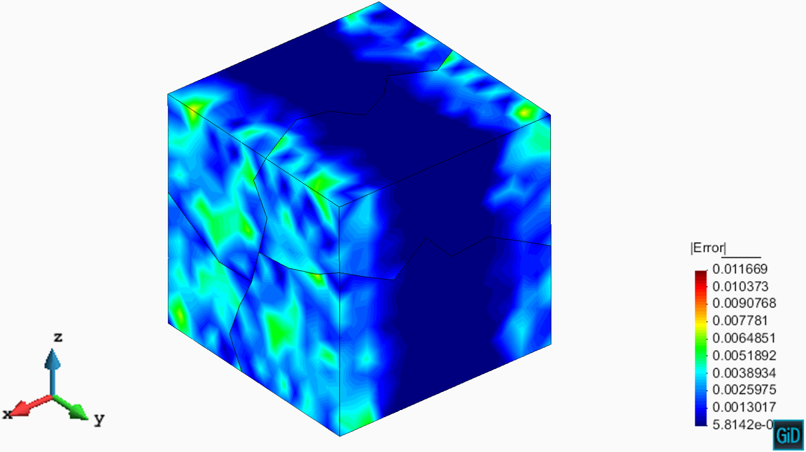

ς_p

DDM

DDM

Formulation

GREMA
RADIOFREQUENCY, ELECTROMAGNETICS, MICROWAVES & ANTENNAS

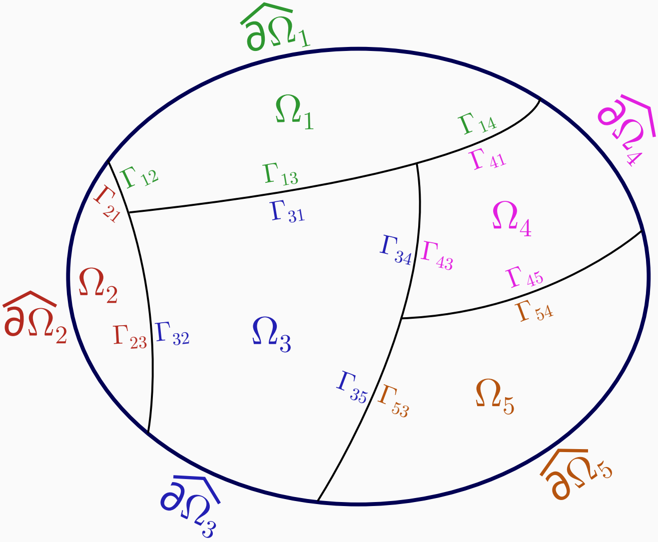

$$\nabla \times \frac{1}{\mu_{ri}}(\nabla \times \mathbf{E}_i) - k_0^2 \varepsilon_{ri} \mathbf{E}_i = \mathbf{O}_i$$

$$\widehat{\mathbf{n}}_i \times \mathbf{E}_i = \mathbf{d}, \text{on } \Gamma_{i,\text{D}};\ \mathbf{d} = 0 \text{ with PEC}$$

$$\widehat{\mathbf{n}}_i \times \frac{1}{\mu_{ri}}(\nabla \times \mathbf{E}_i) = \mathbf{b}, \text{on } \Gamma_{i,\text{N}};\ \mathbf{b} = 0 \text{ with PMC}$$

$$\widehat{\mathbf{n}}_i \times \frac{1}{\mu_{ri}}(\nabla \times \mathbf{E}_i) + jk_0 \widehat{\mathbf{n}}_i \times \widehat{\mathbf{n}}_i \times \mathbf{E}_i = \mathbf{c}, \text{on } \Gamma_{i,\text{C}}$$

$$\boxed{\widehat{\mathbf{n}}_i \times \mathbf{E}_i \times \widehat{\mathbf{n}}_i = \widehat{\mathbf{n}}_j \times \mathbf{E}_j \times \widehat{\mathbf{n}}_j}, \text{on } \Gamma_{ij}$$

$$\boxed{\widehat{\mathbf{n}}_i \times \tfrac{1}{\mu_{ri}}(\nabla \times \mathbf{E}_i) = -\widehat{\mathbf{n}}_j \times \tfrac{1}{\mu_{rj}}(\nabla \times \mathbf{E}_j)}, \text{on } \Gamma_{ij}$$

- Desprès, 1992.
- Three families (2005-):
    - Optimized Schwarz Methods.
    - Cement Element Methods.
    - Finite Element Tearing and Interconnecting techniques.

GREMA RADIOFREQUENCY, ELECTROMAGNETICS, MICROWAVES & ANTENNAS

Transmission conditions:

$$(\alpha\mathcal{I}+\beta_i\mathcal{S}_{\mathsf{TE}})(\mathbf{e}_i) + (\mathcal{I} + \gamma_i\mathcal{S}_{\mathsf{TM}})(\mathbf{j}_i) = (\alpha\mathcal{I} + \beta_j\mathcal{S}_{\mathsf{TE}})(\mathbf{e}_j) - (\mathcal{I} + \gamma_j\mathcal{S}_{\mathsf{TM}})(\mathbf{j}_j)$$

$$\mathcal{S}_{\mathsf{TE}} = \boldsymbol{\nabla}_\tau \times \boldsymbol{\nabla}_\tau \times$$

$$\mathcal{S}_{\mathsf{TM}} = \nabla_\tau \nabla_\tau \cdot$$

Cement variables:

$$\mathbf{e}_i = \widehat{\mathbf{n}}_i \times \mathbf{E}_i \times \widehat{\mathbf{n}}_i$$

$$\mathbf{j}_i = \frac{1}{k_0}\widehat{\mathbf{n}}_i \times \frac{1}{\mu_{ri}}(\boldsymbol{\nabla} \times \mathbf{E}_i)$$

$$\rho_i = \frac{1}{k_0}\nabla_\tau \cdot \mathbf{j}_i$$

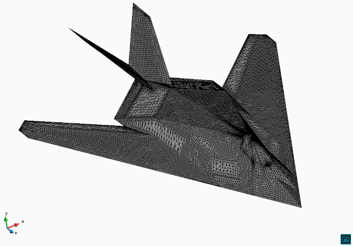

$$\mathbf{Ax} = \mathbf{b}$$

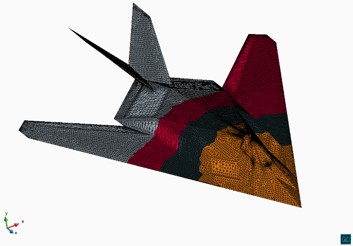

$$\begin{pmatrix} A_1 & C_{12} & \dots & C_{1n} \\ C_{21} & A_2 & \dots & C_{2n} \\ \vdots & \vdots & \ddots & \vdots \\ C_{n1} & C_{n2} & \dots & A_n \end{pmatrix} \begin{pmatrix} \mathbf{x_1} \\ \mathbf{x_2} \\ \vdots \\ \mathbf{x_n} \end{pmatrix} = \begin{pmatrix} \mathbf{b_1} \\ \mathbf{b_2} \\ \vdots \\ \mathbf{b_n} \end{pmatrix}$$

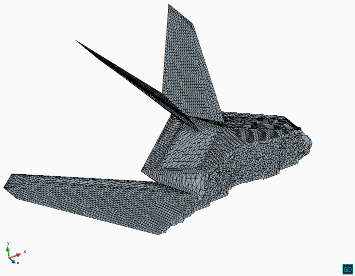

$$\begin{pmatrix} \boxed{A_1} & C_{12} & 0 & 0 \\ C_{21} & A_2 & C_{23} & 0 \\ 0 & C_{32} & A_3 & C_{34} \\ 0 & 0 & C_{43} & A_4 \end{pmatrix} \begin{pmatrix} \boxed{\mathbf{x_1}} \\ \mathbf{x_2} \\ \mathbf{x_3} \\ \mathbf{x_4} \end{pmatrix} = \begin{pmatrix} \boxed{\mathbf{b_1}} \\ \mathbf{b_2} \\ \mathbf{b_3} \\ \mathbf{b_4} \end{pmatrix}$$

DDM: cross matrices

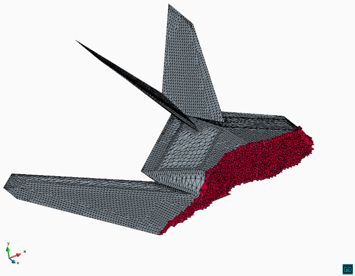

$$\begin{pmatrix} A_1 & \boxed{C_{12}} & 0 & 0 \\ C_{21} & A_2 & C_{23} & 0 \\ 0 & C_{32} & A_3 & C_{34} \\ 0 & 0 & C_{43} & A_4 \end{pmatrix} \begin{pmatrix} \mathbf{x_1} \\ \mathbf{x_2} \\ \mathbf{x_3} \\ \mathbf{x_4} \end{pmatrix} = \begin{pmatrix} \mathbf{b_1} \\ \mathbf{b_2} \\ \mathbf{b_3} \\ \mathbf{b_4} \end{pmatrix}$$

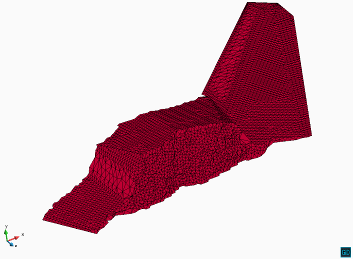

$$\begin{pmatrix} A_1 & C_{12} & 0 & 0 \\ C_{21} & \boxed{A_2} & C_{23} & 0 \\ 0 & C_{32} & A_3 & C_{34} \\ 0 & 0 & C_{43} & A_4 \end{pmatrix} \begin{pmatrix} \mathbf{x_1} \\ \boxed{\mathbf{x_2}} \\ \mathbf{x_3} \\ \mathbf{x_4} \end{pmatrix} = \begin{pmatrix} \mathbf{b_1} \\ \boxed{\mathbf{b_2}} \\ \mathbf{b_3} \\ \mathbf{b_4} \end{pmatrix}$$

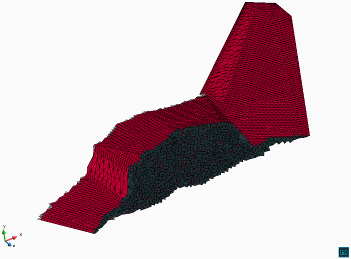

$$\begin{pmatrix} A_1 & C_{12} & 0 & 0 \\ \boxed{C_{21}} & A_2 & \boxed{C_{23}} & 0 \\ 0 & C_{32} & A_3 & C_{34} \\ 0 & 0 & C_{43} & A_4 \end{pmatrix} \begin{pmatrix} \mathbf{x_1} \\ \mathbf{x_2} \\ \mathbf{x_3} \\ \mathbf{x_4} \end{pmatrix} = \begin{pmatrix} \mathbf{b_1} \\ \mathbf{b_2} \\ \mathbf{b_3} \\ \mathbf{b_4} \end{pmatrix}$$

DDM: cross matrices

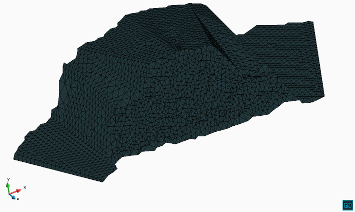

$$\begin{pmatrix} A_1 & C_{12} & 0 & 0 \\ C_{21} & A_2 & C_{23} & 0 \\ 0 & C_{32} & \boxed{A_3} & C_{34} \\ 0 & 0 & C_{43} & A_4 \end{pmatrix} \begin{pmatrix} \mathbf{x_1} \\ \mathbf{x_2} \\ \boxed{\mathbf{x_3}} \\ \mathbf{x_4} \end{pmatrix} = \begin{pmatrix} \mathbf{b_1} \\ \mathbf{b_2} \\ \boxed{\mathbf{b_3}} \\ \mathbf{b_4} \end{pmatrix}$$

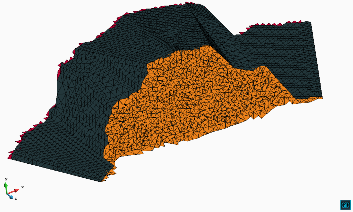

$$\begin{pmatrix} A_1 & C_{12} & 0 & 0 \\ C_{21} & A_2 & C_{23} & 0 \\ 0 & \boxed{C_{32}} & A_3 & \boxed{C_{34}} \\ 0 & 0 & C_{43} & A_4 \end{pmatrix} \begin{pmatrix} \mathbf{x_1} \\ \mathbf{x_2} \\ \mathbf{x_3} \\ \mathbf{x_4} \end{pmatrix} = \begin{pmatrix} \mathbf{b_1} \\ \mathbf{b_2} \\ \mathbf{b_3} \\ \mathbf{b_4} \end{pmatrix}$$

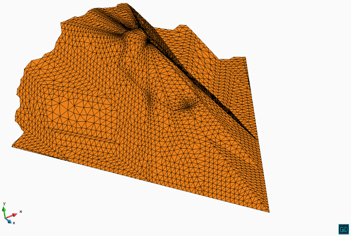

$$\begin{pmatrix} A_1 & C_{12} & 0 & 0 \\ C_{21} & A_2 & C_{23} & 0 \\ 0 & C_{32} & A_3 & C_{34} \\ 0 & 0 & C_{43} & \boxed{A_4} \end{pmatrix} \begin{pmatrix} \mathbf{x_1} \\ \mathbf{x_2} \\ \mathbf{x_3} \\ \boxed{\mathbf{x_4}} \end{pmatrix} = \begin{pmatrix} \mathbf{b_1} \\ \mathbf{b_2} \\ \mathbf{b_3} \\ \boxed{\mathbf{b_4}} \end{pmatrix}$$

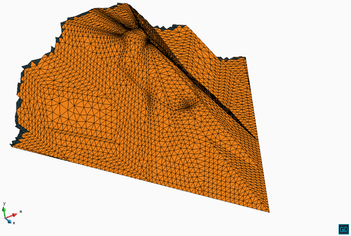

$$\begin{pmatrix} A_1 & C_{12} & 0 & 0 \\ C_{21} & A_2 & C_{23} & 0 \\ 0 & C_{32} & A_3 & C_{34} \\ 0 & 0 & \boxed{C_{43}} & A_4 \end{pmatrix} \begin{pmatrix} \mathbf{x_1} \\ \mathbf{x_2} \\ \mathbf{x_3} \\ \mathbf{x_4} \end{pmatrix} = \begin{pmatrix} \mathbf{b_1} \\ \mathbf{b_2} \\ \mathbf{b_3} \\ \mathbf{b_4} \end{pmatrix}$$

Block Jacobi:

$$M = \begin{pmatrix} A_1 & \dots & 0 \\ \vdots & \ddots & \vdots \\ 0 & \dots & A_n \end{pmatrix}, N = \begin{pmatrix} 0 & \dots & -C_{1n} \\ \vdots & \ddots & \vdots \\ -C_{n1} & \dots & 0 \end{pmatrix}$$

$$M^{-1}A = \mathcal{I} - M^{-1}N = \begin{pmatrix} \mathcal{I} & \dots & A_1^{-1}C_{1n} \\ \vdots & \ddots & \vdots \\ A_n^{-1}C_{n1} & \dots & \mathcal{I} \end{pmatrix}$$

Three level parallelization:

- Algorithm: DDM.
- Process: MPI.
- Thread: OpenMP.

DDM

Verification

- Introduction of domains: user-driven or ParMETIS.

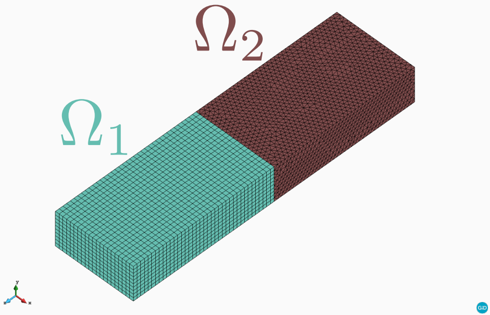

- Introduction of domains: user-driven or ParMETIS.

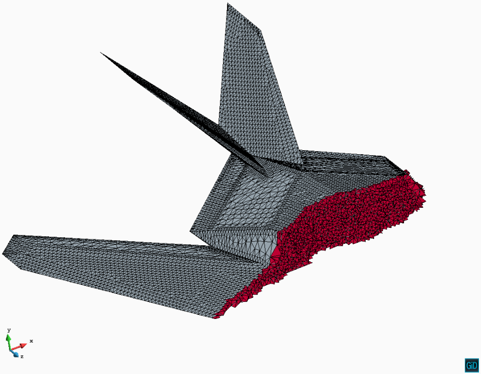

- Introduction of domains: user-driven or ParMETIS.
- Non-matching interfaces.

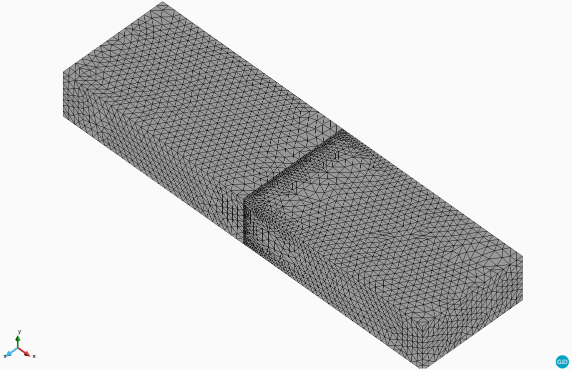

- Introduction of domains: user-driven or ParMETIS.
- Non-matching interfaces.
- Shapes.

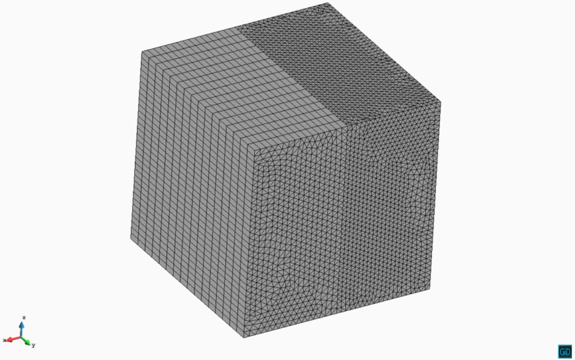

- Introduction of domains: user-driven or ParMETIS.
- Non-matching interfaces.
- Orders.

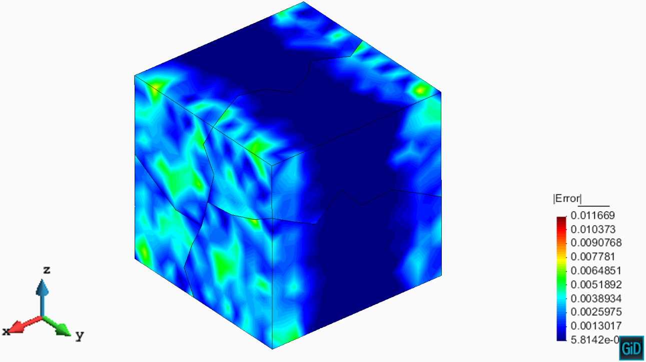

- Two-step procedure:
    1. Move C_{ij} to the RHS introducing $\mathbf{E}$ and cement variables.

$$\begin{pmatrix} A_1 & 0 & 0 & 0 \\ 0 & A_2 & 0 & 0 \\ 0 & 0 & A_3 & 0 \\ 0 & 0 & 0 & A_4 \end{pmatrix} \begin{pmatrix} \mathbf{x_1} \\ \mathbf{x_2} \\ \mathbf{x_3} \\ \mathbf{x_4} \end{pmatrix} = \begin{pmatrix} \mathbf{b_1} - C_{12}\mathbf{x}_{2,\text{MMS}} \\ \mathbf{b_2} - C_{21}\mathbf{x}_{1,\text{MMS}} - C_{23}\mathbf{x}_{3,\text{MMS}} \\ \mathbf{b_3} - C_{32}\mathbf{x}_{2,\text{MMS}} - C_{34}\mathbf{x}_{4,\text{MMS}} \\ \mathbf{b_4} - C_{43}\mathbf{x}_{3,\text{MMS}} \end{pmatrix}$$

- Two-step procedure:
    1. Move C_{ij} to the RHS introducing $\mathbf{E}$ and cement variables.
    2. Introduce only $\mathbf{E}$ as manufactured solution.

DDM: non-conformal in shape and order

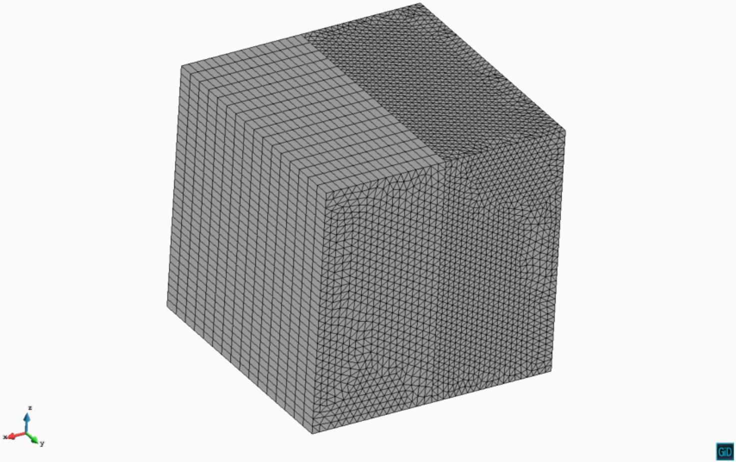

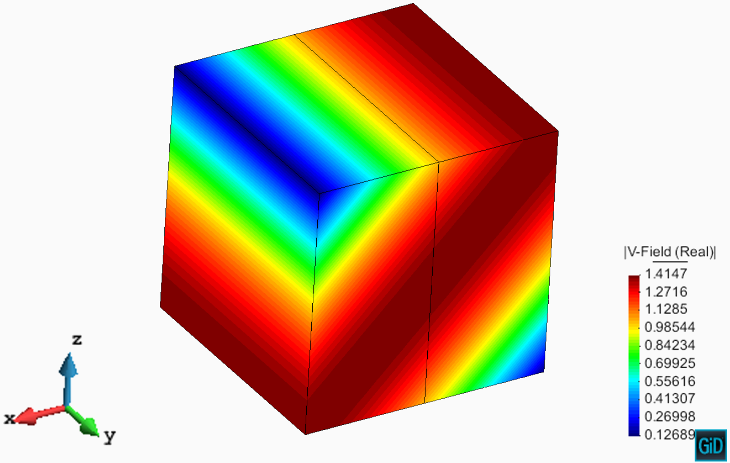
|V-Field (Real)|
1.4147
1.2716
1.1285
0.98544
0.84234
0.69925
0.55616
0.41307
0.26998
0.12689
GiD
z
x
y

DDM: non-conformal in shape and order

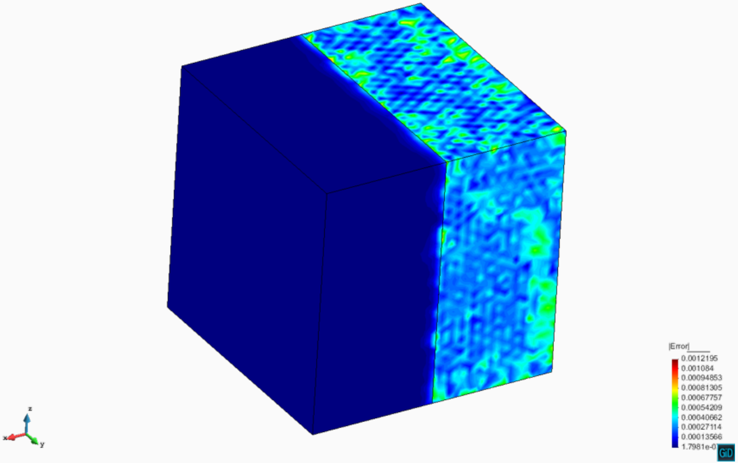

Preconditioned surface problem:

$$M^{-1}A = \mathcal{I} - M^{-1}N = \begin{pmatrix} \mathcal{I} & \dots & A_1^{-1}C_{1n} \\ \vdots & \ddots & \vdots \\ A_n^{-1}C_{n1} & \dots & \mathcal{I} \end{pmatrix}$$

Transmission conditions:

$$(\alpha\mathcal{I}+\beta_i\mathcal{S}_{\mathsf{TE}})(\mathbf{e}_i) + (\mathcal{I} + \gamma_i\mathcal{S}_{\mathsf{TM}})(\mathbf{j}_i) = (\alpha\mathcal{I} + \beta_j\mathcal{S}_{\mathsf{TE}})(\mathbf{e}_j) - (\mathcal{I} + \gamma_j\mathcal{S}_{\mathsf{TM}})(\mathbf{j}_j)$$

DDM: eigenspectra

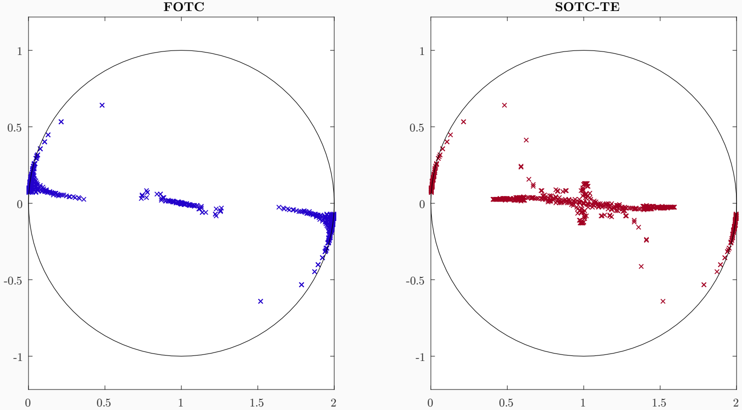

- 2D array of circular horns.
- WR-90 waveguides, $f = 10\,\text{GHz}$.

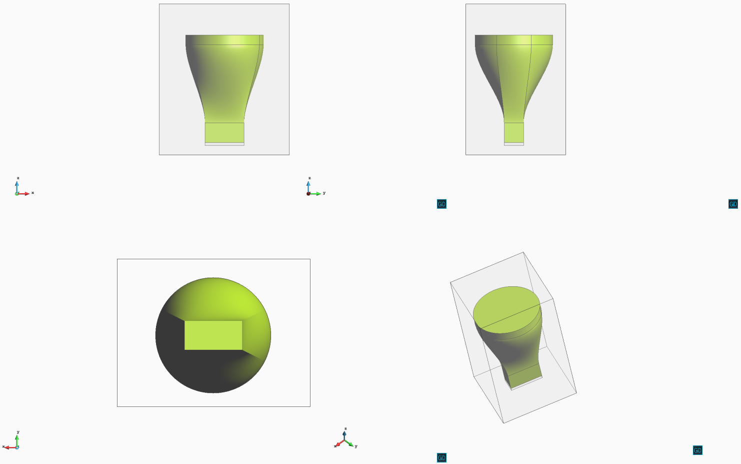

DDM: 2D partitioning

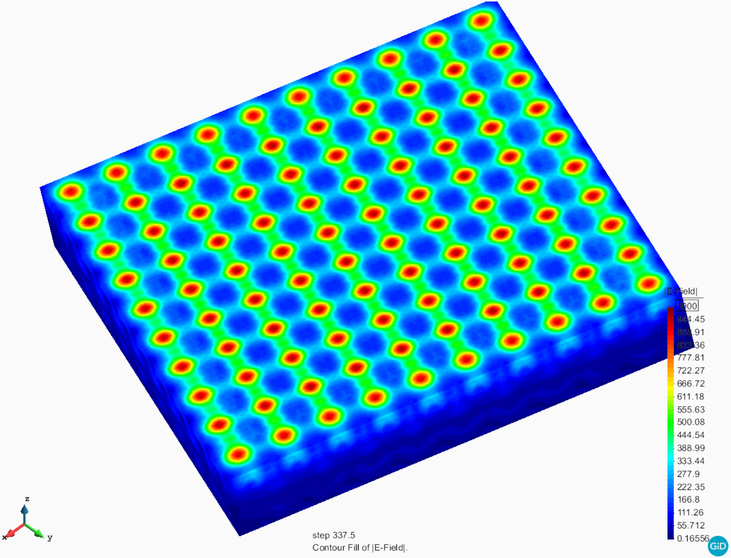

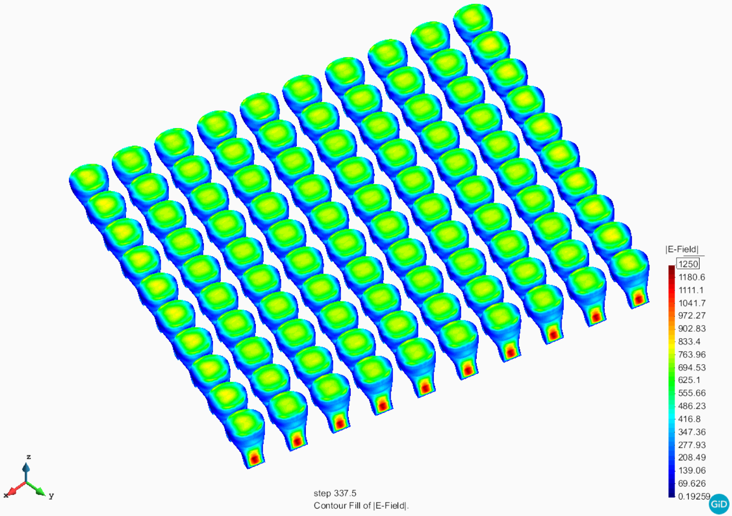

|E-Field|
1250
1180.6
1111.1
1041.7
972.27
902.83
833.4
763.96
694.53
625.1
555.66
486.23
416.8
347.36
277.93
208.49
139.06
69.626
0.19259
z
x
y
step 337.5
Contour Fill of |E-Field|.
GiD

- RCS of stealth fighter (F117).
- 10 METIS domains.

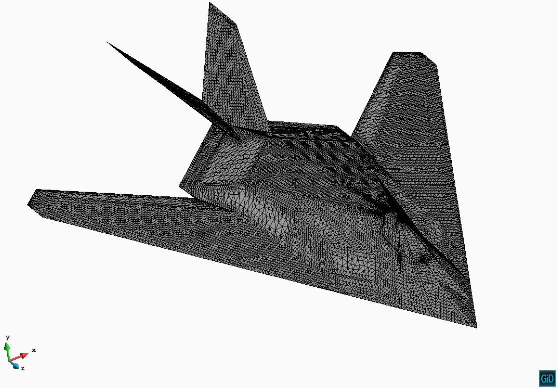

- RCS of stealth fighter (F117).
- 10 METIS domains.

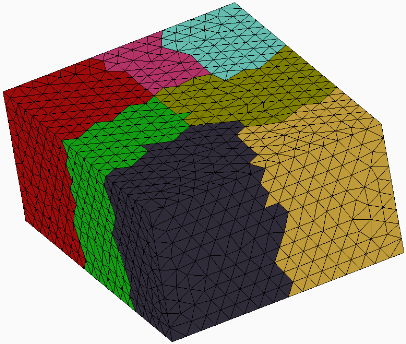

DDM: 3D partitioning

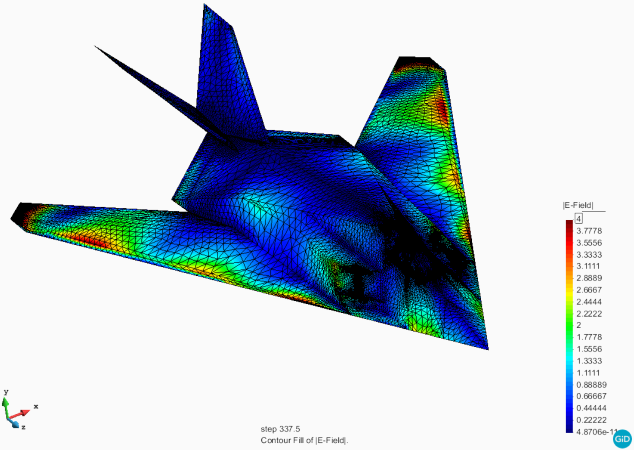

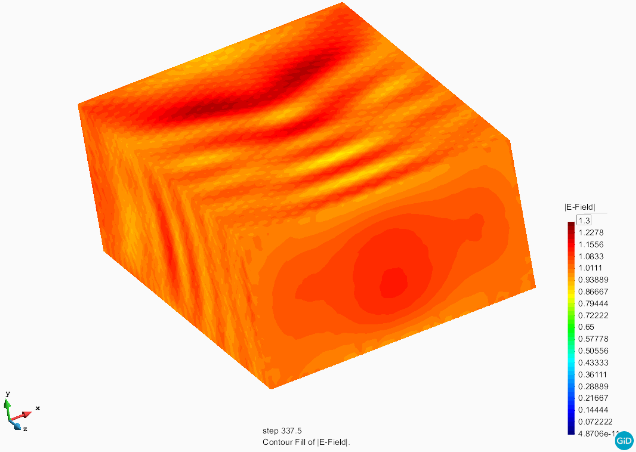
|E-Field|
1.3
1.2278
1.1556
1.0833
1.0111
0.93889
0.86667
0.79444
0.72222
0.65
0.57778
0.50556
0.43333
0.36111
0.28889
0.21667
0.14444
0.072222
4.8706e-11
y
x
z
step 337.5
Contour Fill of |E-Field|.
GiD

DDM: 3D partitioning

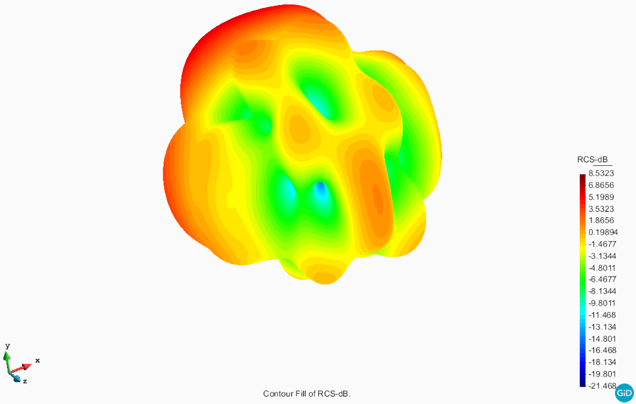

Contour Fill of RCS-dB.

Problem to be solved:

- WR-90 waveguide.
- 0.5λ sections per domain.

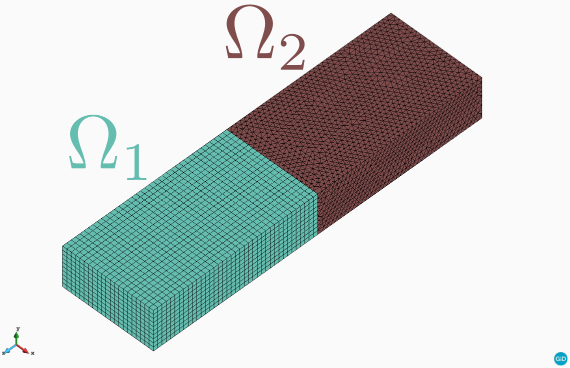

h refinement?

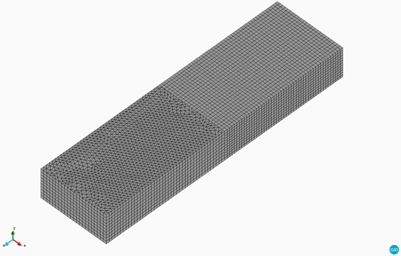

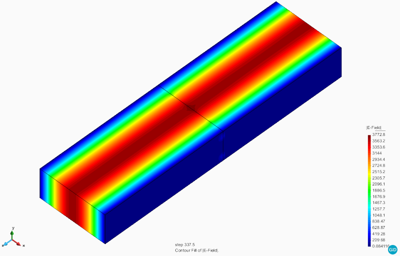

$$|s_{21}| = 0.999995$$

h refinement?

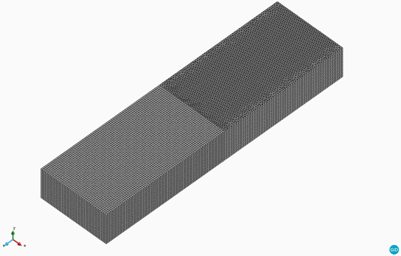

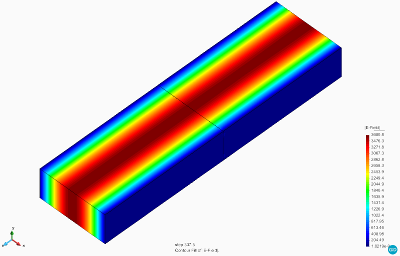

$$|s_{21}| = 0.999999$$

Aspect ratio?

- Same mesh on the waveports.

Aspect ratio?

- Same mesh on the waveports.
- Tetrahedra: only changes on the interface.

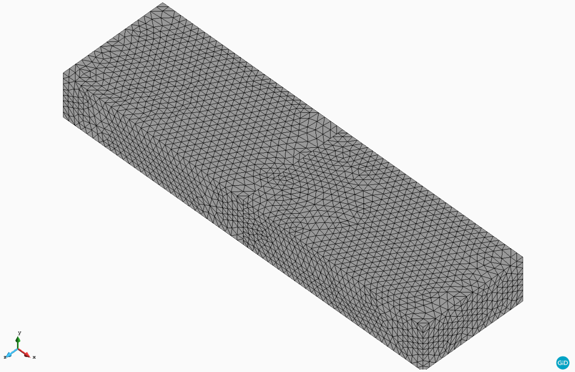

Aspect ratio?

- Same mesh on the waveports.
- Tetrahedra: only changes on the interface.

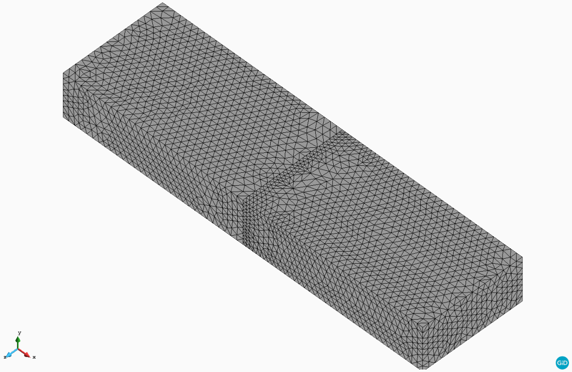

Aspect ratio?

- Same mesh on the waveports.
- Tetrahedra: only changes on the interface.

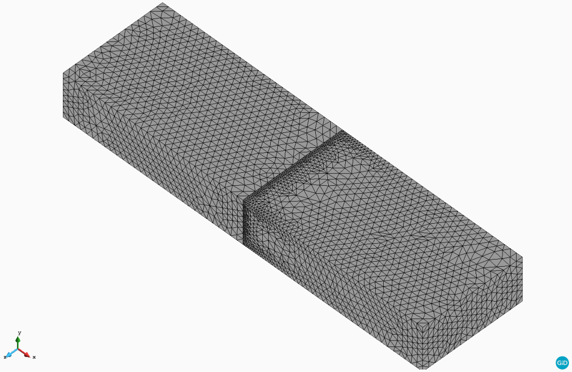

Aspect ratio?

- Same mesh on the waveports.
- Triangular prisms: three sections.

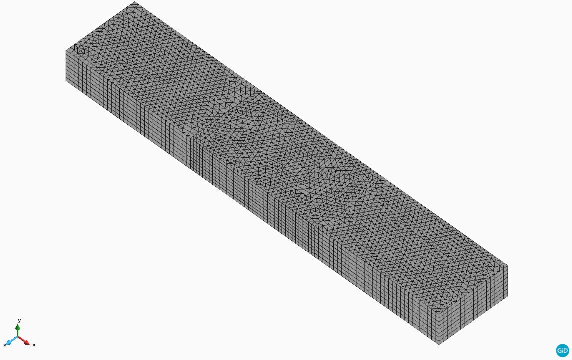

Aspect ratio?

- Same mesh on the waveports.
- Triangular prisms: three sections.

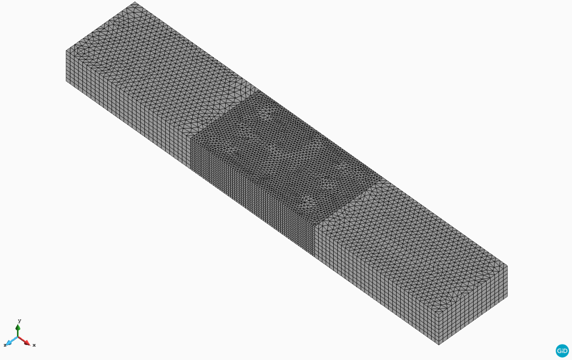

Aspect ratio?

- Same mesh on the waveports.
- Triangular prisms: three sections.

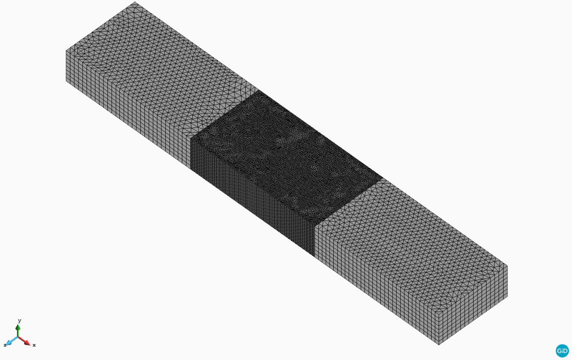

GREMA
RADIOFREQUENCY, ELECTROMAGNETICS, MICROWAVES & ANTENNAS

Aspect ratio?

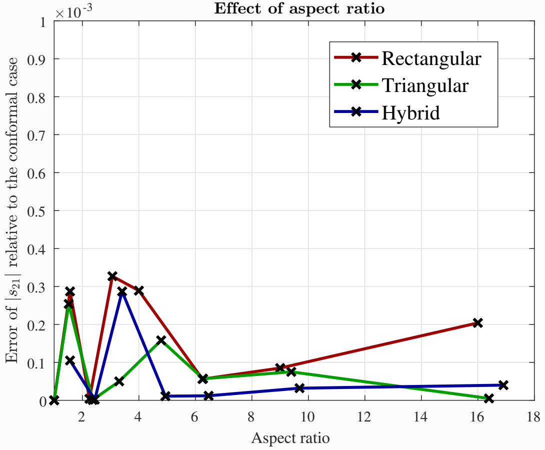

GREMA
RADIOFREQUENCY, ELECTROMAGNETICS, MICROWAVES & ANTENNAS

Aspect ratio?

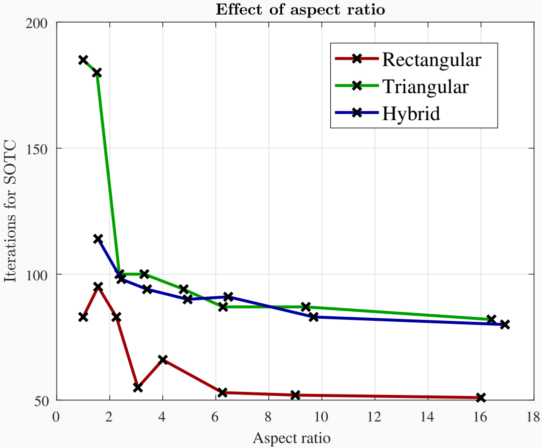

Number of discontinuities?

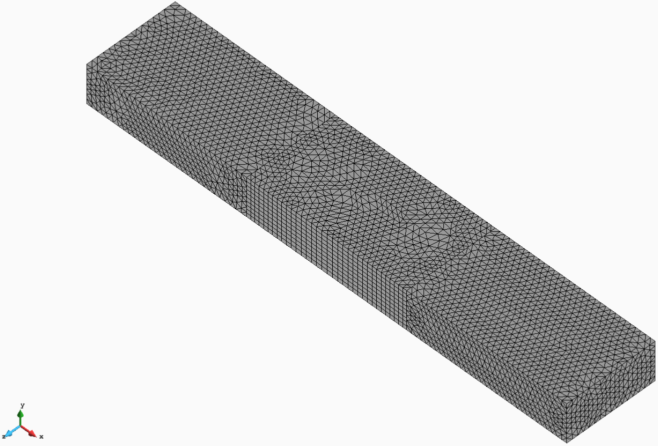

GREMA
RADIOFREQUENCY, ELECTROMAGNETICS, MICROWAVES & ANTENNAS

Number of discontinuities?

Number of discontinuities?

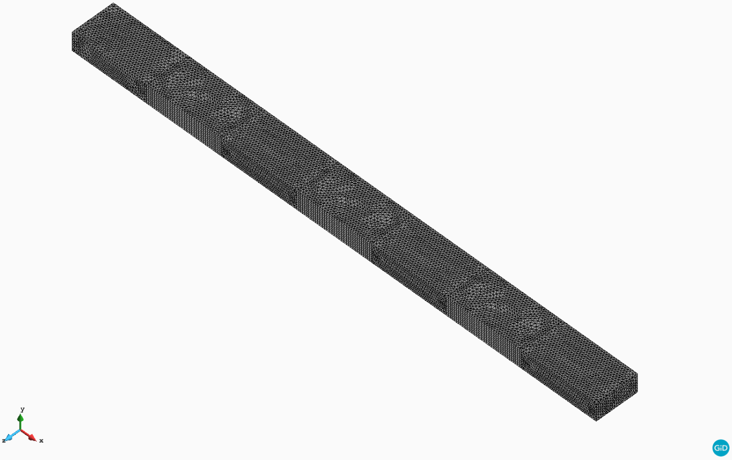

Number of discontinuities?

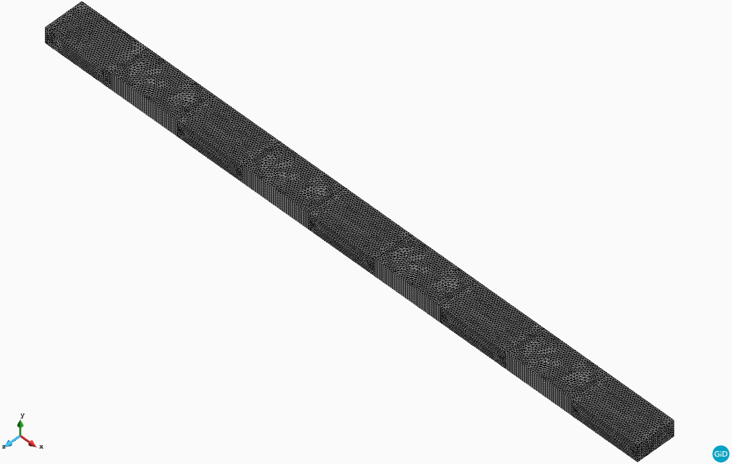

Number of discontinuities?

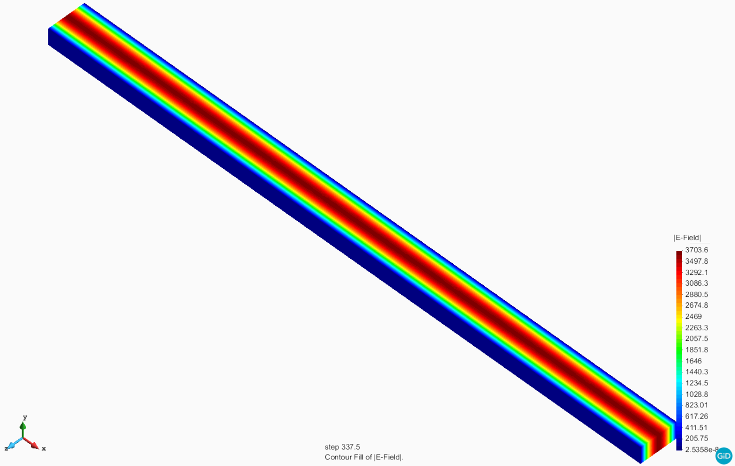

GREMA
RADIOFREQUENCY, ELECTROMAGNETICS, MICROWAVES & ANTENNAS

Number of discontinuities?

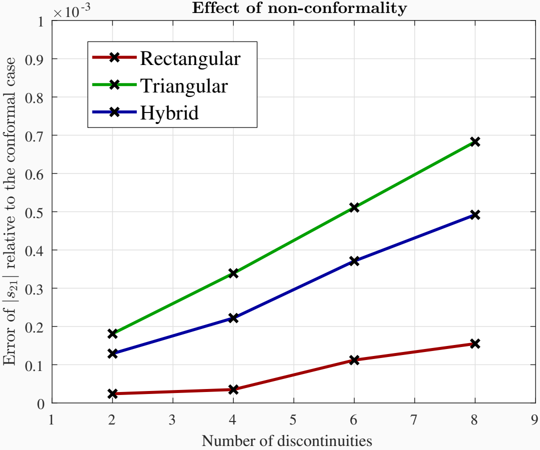

Number of discontinuities?

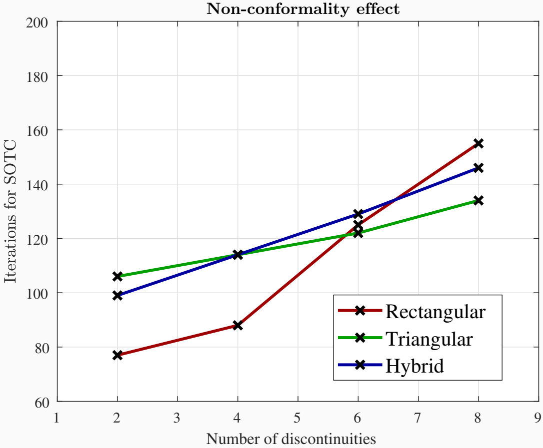

Adaptivity

Adaptivity: building blocks

Building blocks:

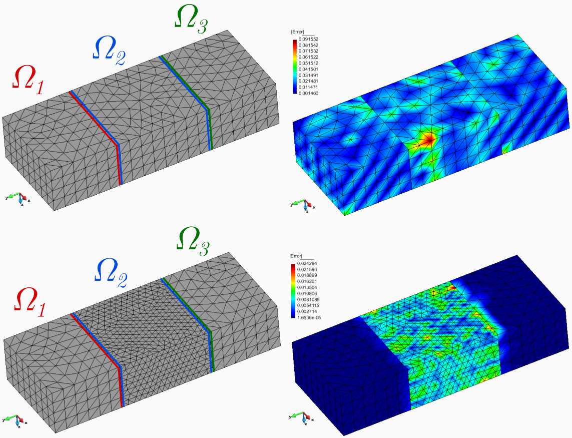

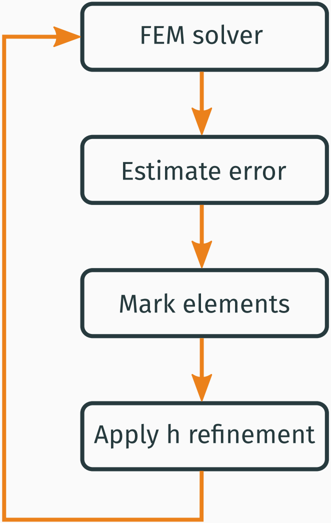
FEM solver
Estimate error
Mark elements
Apply h refinement

Adaptivity

Algorithm

Estimator based on residuals:

- Volume,

$$\mathcal{R}_{\text{vol},i}^{(m)} = \boldsymbol{\nabla} \times \mu_{ri}^{-1}(\boldsymbol{\nabla} \times \mathbf{E}_{i,\text{FEM}}^{(m)}) - k_0^2 \varepsilon_{ri} \mathbf{E}_{i,\text{FEM}}^{(m)} - \mathbf{O}_i.$$

Botha, M. M., and Davidson, D. B. (2005). "An explicit a posteriori error indicator for electromagnetic, finite element-boundary integral analysis.", *IEEE Transactions on antennas and propagation*, 53(11), 3717-3725.

GREMA RADIOFREQUENCY, ELECTROMAGNETICS, MICROWAVES & ANTENNAS

Estimator based on residuals:

- Boundary conditions,

$$\mathcal{R}_{\mathsf{D}}^{(m)} = 0, \quad \text{on } \Gamma_{i,\mathsf{D}}, \tag{1}$$

$$\mathcal{R}_{\mathsf{N}}^{(m)} = \widehat{\mathbf{n}}_i^{(m)} \times \mu_{ri}^{-1}(\boldsymbol{\nabla} \times \mathbf{E}_{i,\mathsf{FEM}}^{(m)}), \quad \text{on } \Gamma_{i,\mathsf{N}}, \tag{2}$$

$$\mathcal{R}_{\mathsf{C}}^{(m)} = \widehat{\mathbf{n}}_i \times \mu_{ri}^{-1}(\boldsymbol{\nabla} \times \mathbf{E}_{i,\mathsf{FEM}}^{(m)}) + jk_0\widehat{\mathbf{n}}_i^{(m)} \times \widehat{\mathbf{n}}_i^{(m)} \times (\boldsymbol{\Psi}_i - \mathbf{E}_{i,\mathsf{FEM}}^{(m)}), \quad \text{on } \Gamma_{i,\mathsf{C}}. \tag{3}$$

Estimator based on residuals:

- Neighbor elements,

$$\mathcal{R}_{i,\text{neigh}}^{(m)} = \widehat{\mathbf{n}}_i^{(m)} \times \mu_{ri}^{-1}(\boldsymbol{\nabla} \times \mathbf{E}_{i,\text{FEM}}^{(m)}) + \widehat{\mathbf{n}}_i^{(n)} \times \mu_{ri}^{-1}(\boldsymbol{\nabla} \times \mathbf{E}_{i,\text{FEM}}^{(n)}).$$

Estimator based on residuals:

- DDM interfaces,

$$\mathcal{R}_{ij,\mathsf{DDM}}^{(m)} = \pi_\tau(\mathbf{E}_{i,\mathsf{FEM}}^{(m)}) + \pi_\tau^\times(\mu_{ri}^{-1}\boldsymbol{\nabla} \times \mathbf{E}_{i,\mathsf{FEM}}^{(m)}) - \pi_\tau(\mathbf{E}_{j,\mathsf{FEM}}^{(n)}) - \pi_\tau^\times(\mu_{rj}^{-1}\boldsymbol{\nabla} \times \mathbf{E}_{j,\mathsf{FEM}}^{(n)}).$$

Five marking strategies are coded.

- Based on a threshold of the maximum.

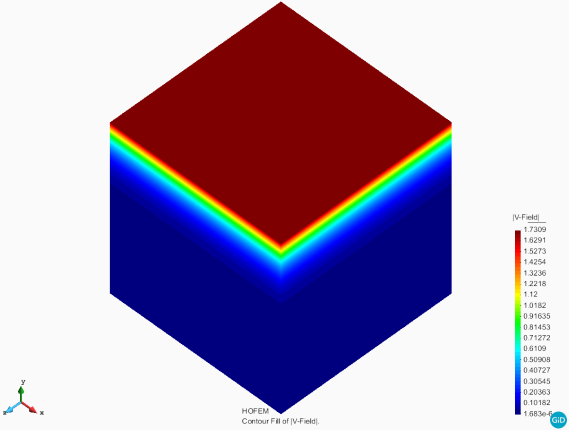

Five marking strategies are coded.

- Based on a threshold of the maximum.

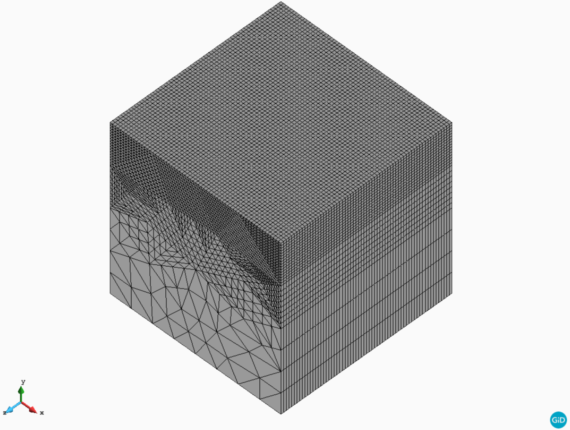

Refinement based on red-green-red:

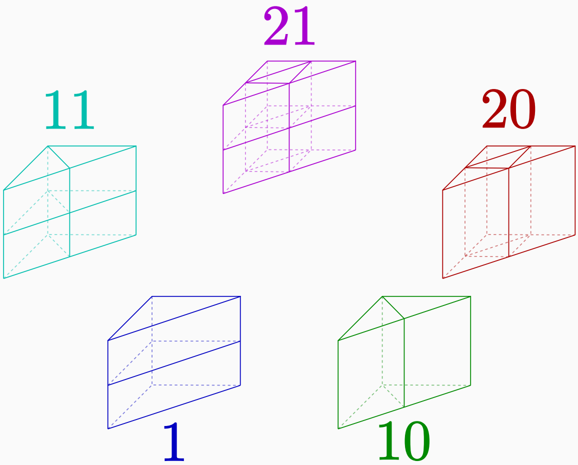

Propagation to avoid hanging nodes:

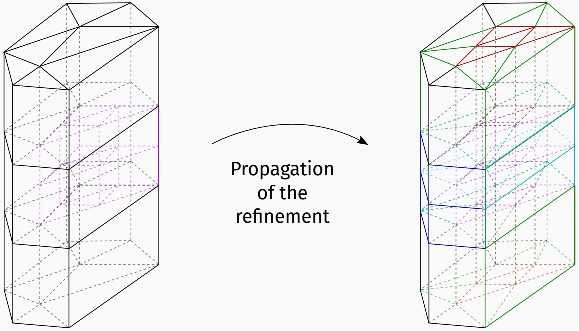

Adaptivity

Validation with DDM

Validation with a WR-90 waveguide:

- Structured prismatic mesh.
- $f = 7.5$ GHz.
- No DDM.

Adaptivity: validation

Validation with a WR-90 waveguide:

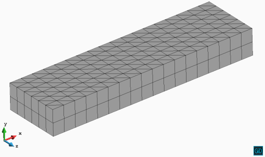

Mesh

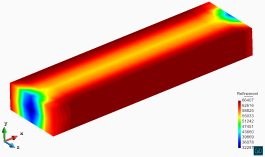

Estimator

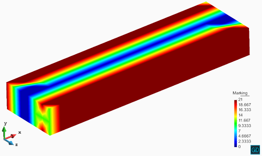

Marking

Adaptivity: validation

Validation with a WR-90 waveguide:

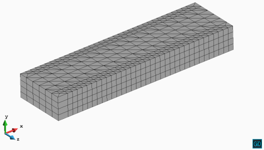

Mesh

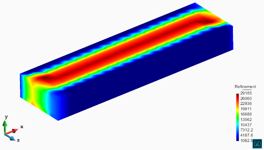

Estimator

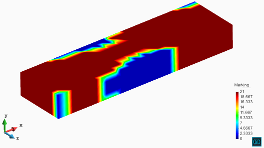

Marking

GREMA
RADIOFREQUENCY, ELECTROMAGNETICS, MICROWAVES & ANTENNAS

Validation with a WR-90 waveguide:

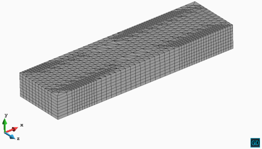

Mesh

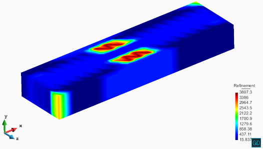

Estimator

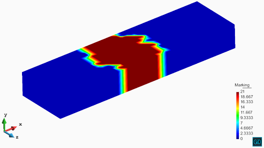

Marking

GREMA
RADIOFREQUENCY, ELECTROMAGNETICS, MICROWAVES & ANTENNAS

Validation with a WR-90 waveguide:

- Unstructured mesh,

$$\varsigma_{\text{wg}} = \boldsymbol{\nabla} \times \mu_{ri}^{-1}(\boldsymbol{\nabla} \times \mathbf{E}_h) - k_0^2 \varepsilon_{ri} \mathbf{E}_h,$$

$$\mathbf{E}_h = \mathbf{E} - \mathbf{E}_{\text{anal}}.$$

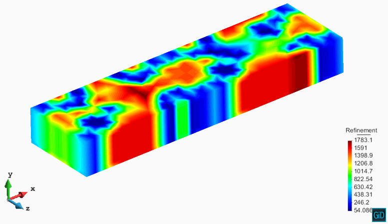

Estimator

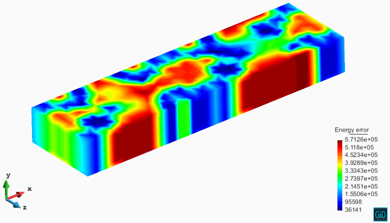

ς_{wg}

GREMA
RADIOFREQUENCY, ELECTROMAGNETICS, MICROWAVES & ANTENNAS

Validation with a WR-90 waveguide:

- Introduction of DDM with matching interfaces.

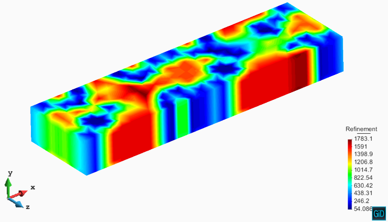

No DDM

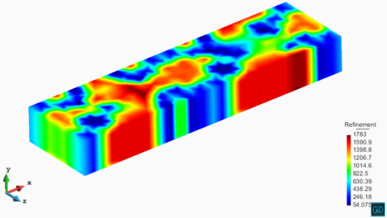

DDM with conf. mesh

Refinement with DDM and non-conformal mesh:

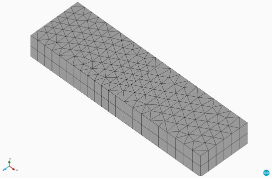

Mesh

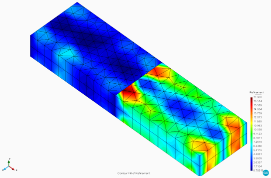

Estimator

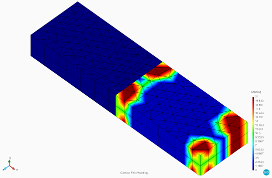

Marking

Refinement with DDM and non-conformal mesh:

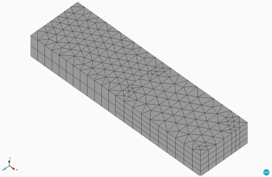

Mesh

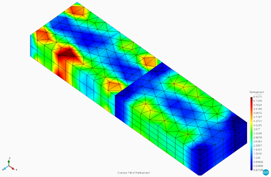

Estimator

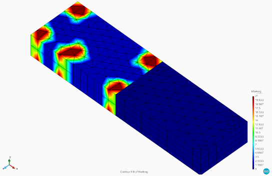

Marking

Adaptivity: non-conformal DDM

GREMA
RADIOFREQUENCY, ELECTROMAGNETICS, MICROWAVES & ANTENNAS

Refinement with DDM and non-conformal mesh:

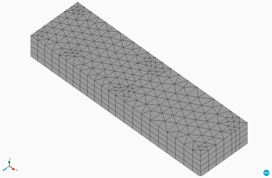

Mesh

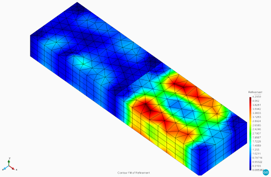

Estimator

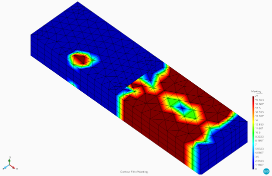

Marking

Adaptivity

L-shaped waveguides

Bend along H-plane in a waveguide:

- Three domains.
- $a = 2b$, $f = f_{c,\text{TE10}}$.

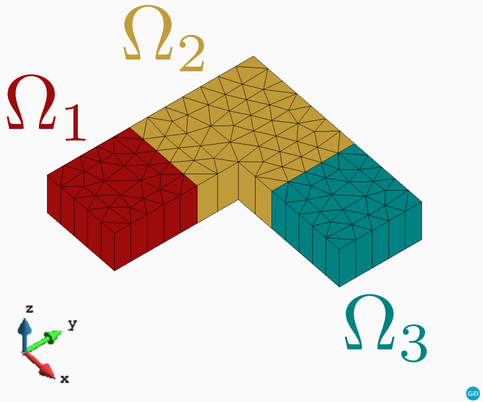

Bend along H-plane in a waveguide:

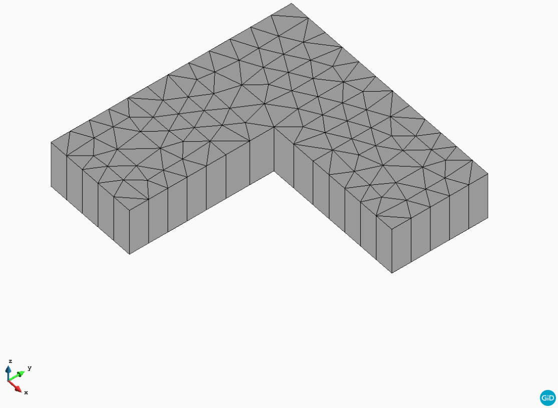

Bend along H-plane in a waveguide:

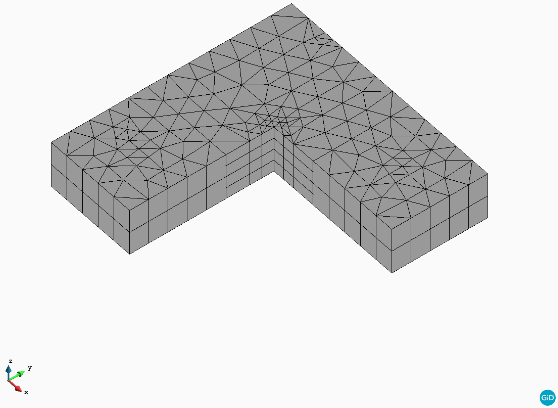

Bend along H-plane in a waveguide:

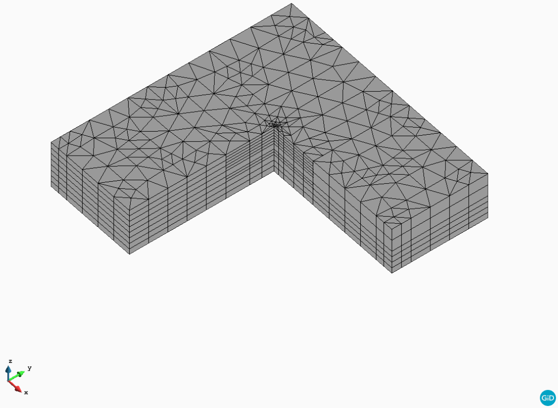

Bend along H-plane in a waveguide:

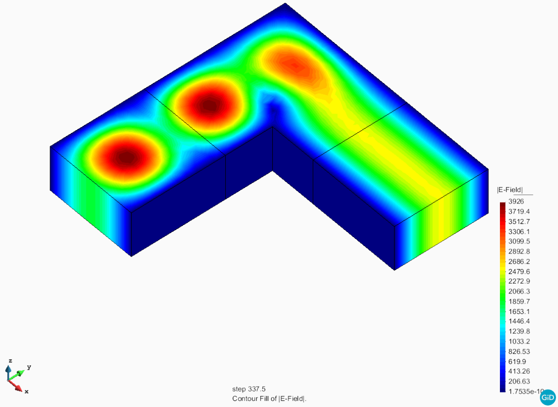

GREMA
RADIOFREQUENCY, ELECTROMAGNETICS, MICROWAVES & ANTENNAS

Bend along H-plane in a waveguide:

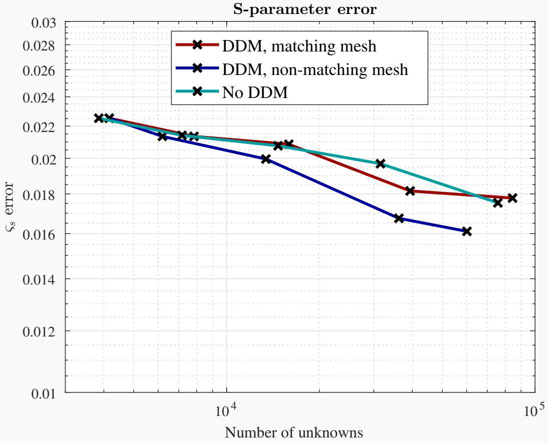

Bend along H-plane in a waveguide:

$$\varsigma_s = \frac{|s_{\mathsf{FEM}} - s_{\mathsf{MM}}|}{|s_{\mathsf{MM}}} \tag{1}$$

Bend along E-plane in a WR-90 waveguide:

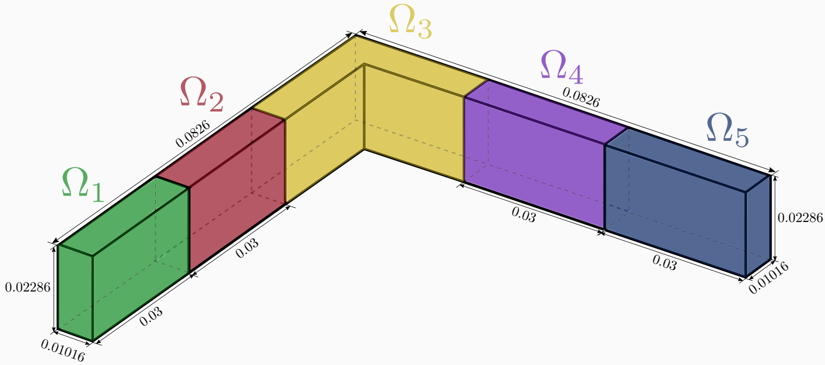

Experiments:

1. Uniform refinement.

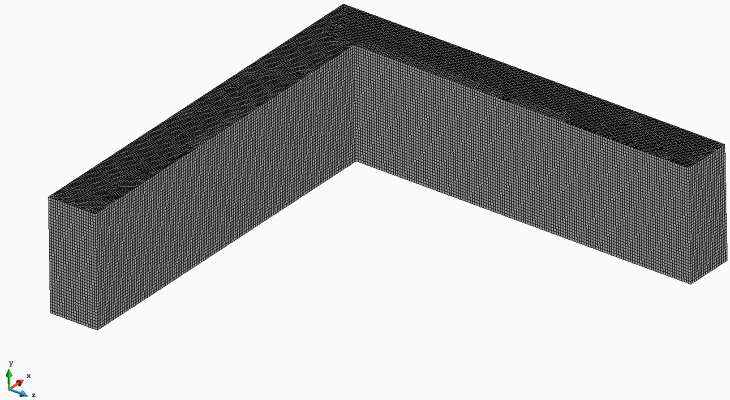

Adaptivity: bend along E-plane

Experiments:

1. Uniform refinement.

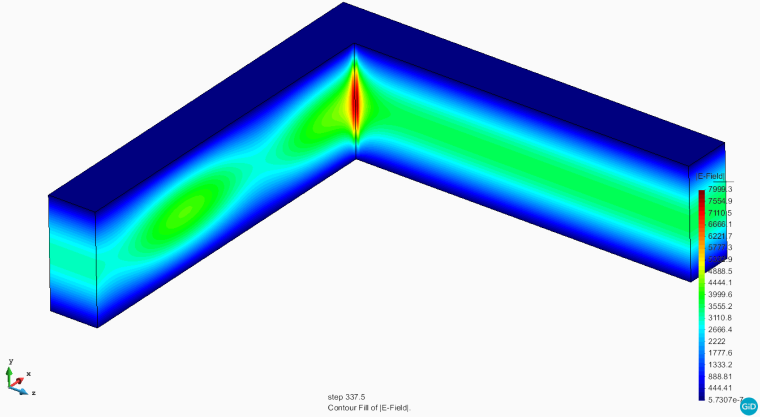

Experiments:

2. *h* refinement with DDM and conformal meshes.

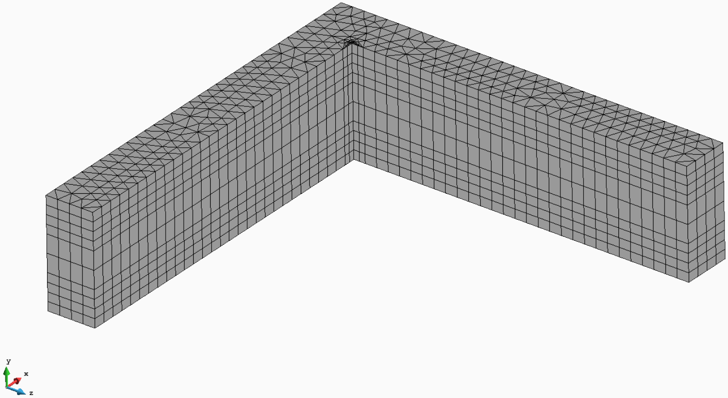

Adaptivity: bend along E-plane

Experiments:

2. *h* refinement with DDM and conformal meshes.

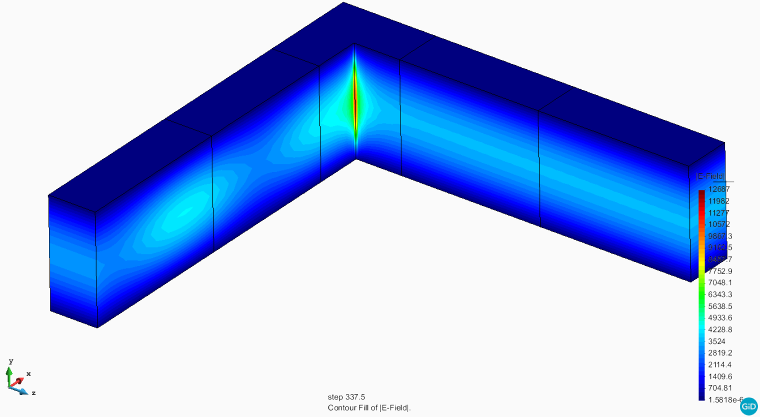

Experiments:

3. *h* refinement with $p = 3$ in some parts.

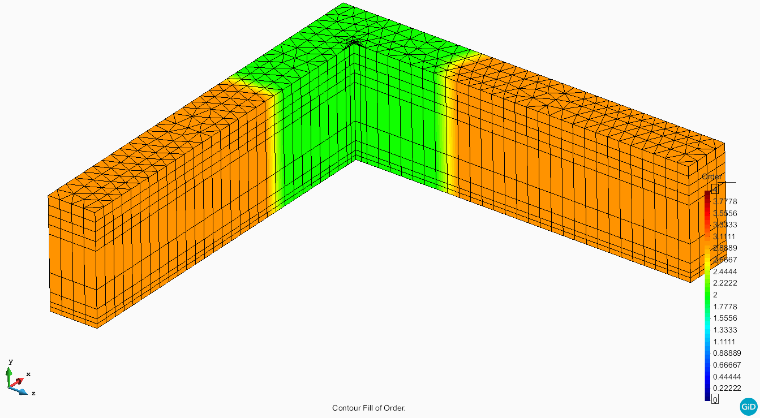

Contour Fill of Order.

GREMA
RADIOFREQUENCY, ELECTROMAGNETICS, MICROWAVES & ANTENNAS

Experiments:

3. h refinement with $p = 3$ in some parts.

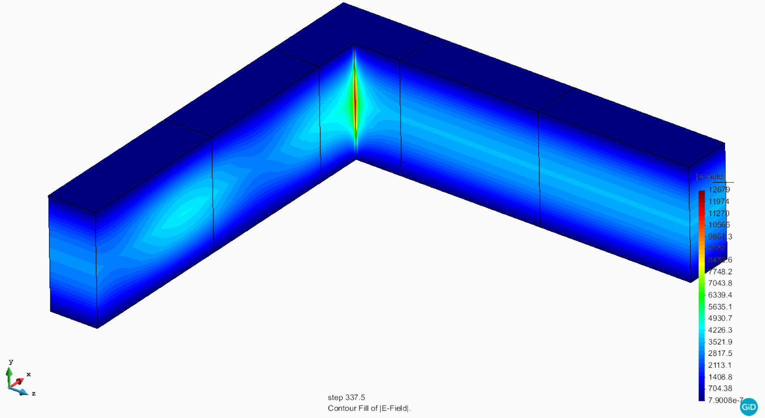

Adaptivity: bend along E-plane

Experiments:

4. *h* refinement with *p* refinement.

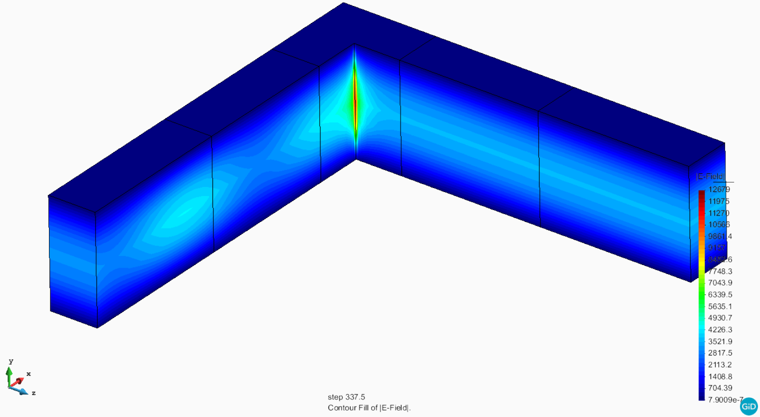

Experiments:

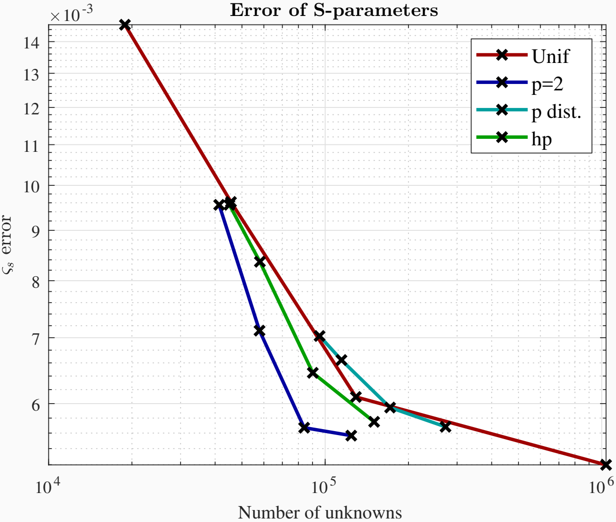

Experiments:

5. *h* refinement with DDM and non-matching meshes.

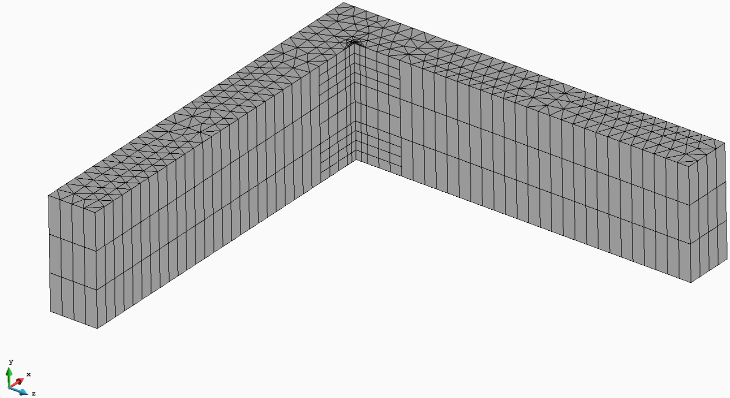

Adaptivity: bend along E-plane

Experiments:

5. *h* refinement with DDM and non-matching meshes.

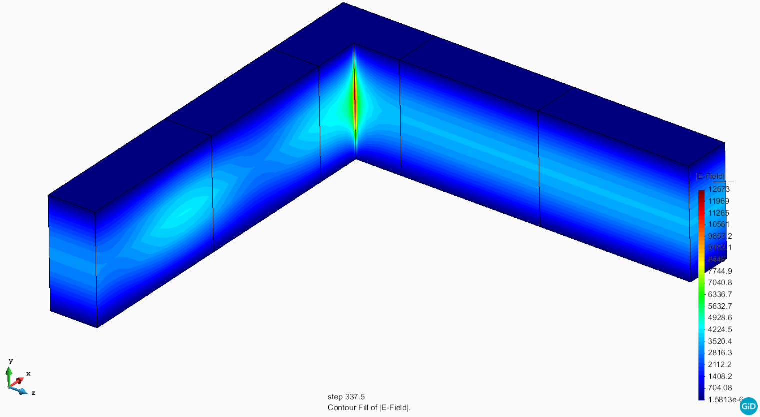

Experiments:

2. *h* refinement with DDM and matching meshes.

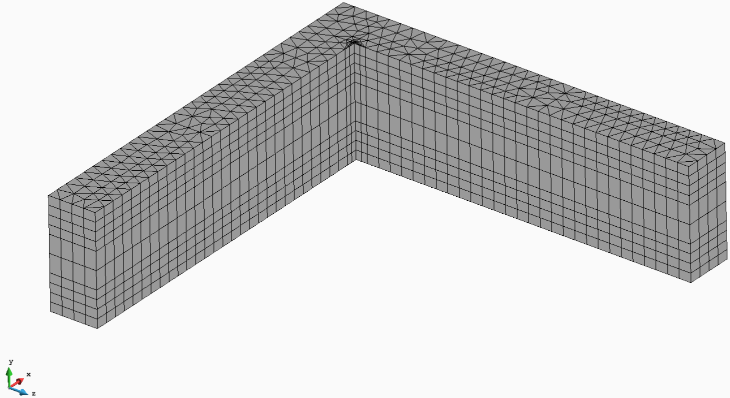

Experiments:

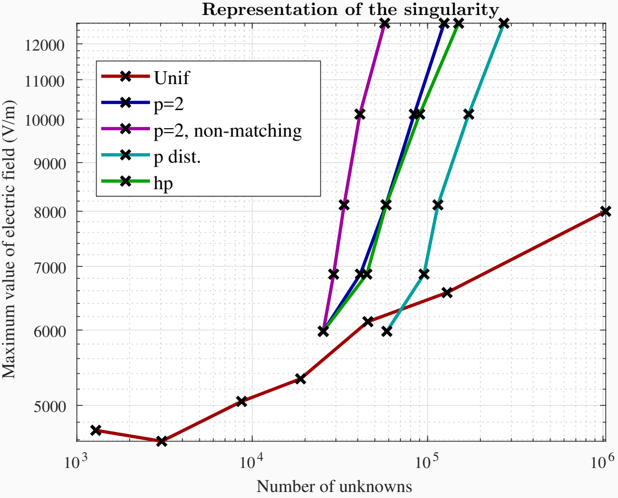

Adaptivity

Towards real adaptivity

Real problem (Slotted Waveguide Array):

- Resonant SWA with length $4.5\lambda_g$.
- 7 elliptical slots.
- 9 subdomains.
- Working frequency: $f = 3.4045$ GHz.

El Misilmani, Hilal M., Mohammed Al-Husseini, and Karim Y. Kabalan. ”Design of slotted waveguide antennas with low sidelobes for high power microwave applications.” *Progress In Electromagnetics Research* 56 (2015): 15-28.

Real problem (Slotted Waveguide Array):

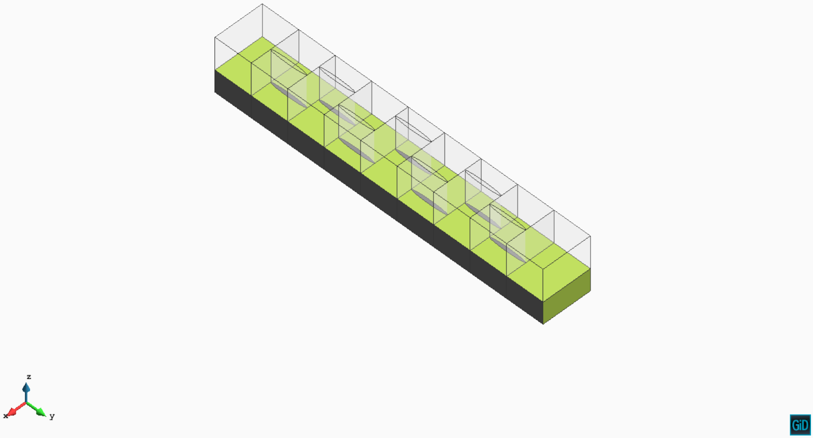

GREMA
RADIOFREQUENCY, ELECTROMAGNETICS, MICROWAVES & ANTENNAS

Real problem (Slotted Waveguide Array):

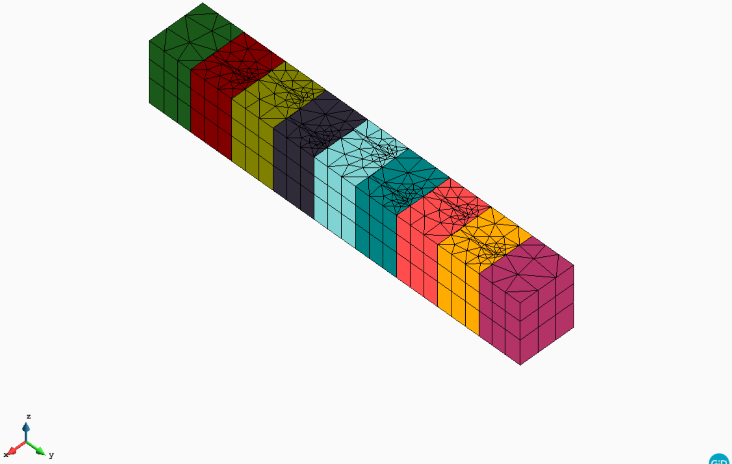

Real problem (Slotted Waveguide Array):

	Matching interfaces		*Non-matching interfaces*	
Round	# elements	# unknowns	# elements	# unknowns
1	1482	26644	1482	26644
1	5694	93236	2278	39110
2	37464	568636	7758	122292
3	79704	1196226	32747	493358

Real problem (Slotted Waveguide Array):

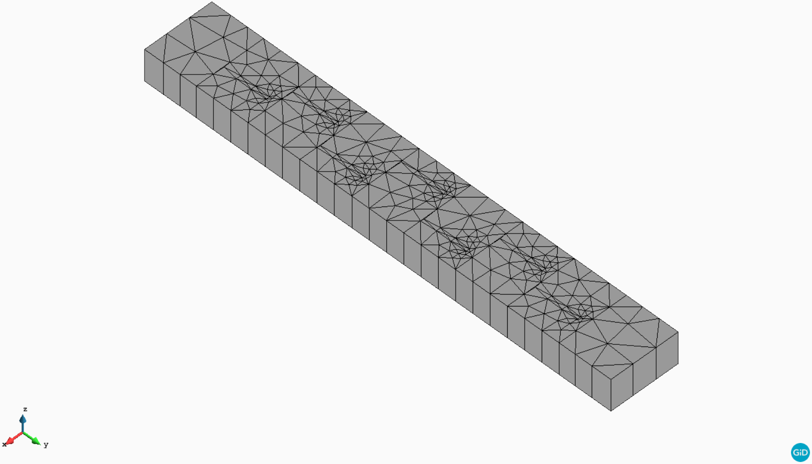

Real problem (Slotted Waveguide Array):

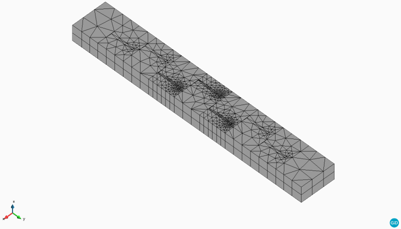

Matching mesh

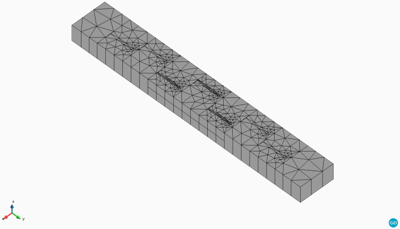

Non-matching mesh

GREMA RADIOFREQUENCY, ELECTROMAGNETICS, MICROWAVES & ANTENNAS

Real problem (Slotted Waveguide Array):

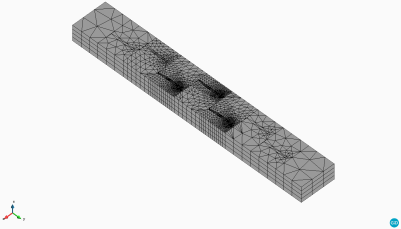

Matching mesh

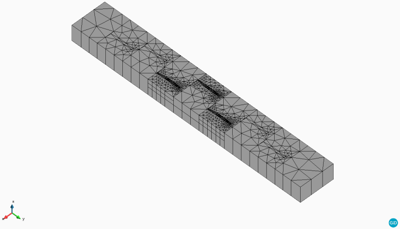

Non-matching mesh

Real problem (Slotted Waveguide Array):

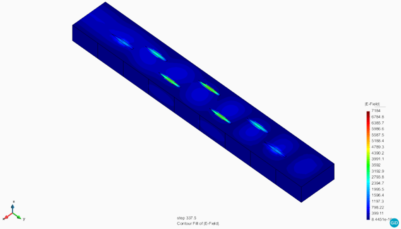

Matching mesh

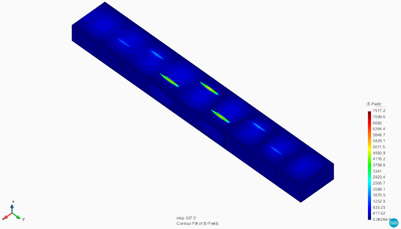

Non-matching mesh

Conclusions and future lines

Conclusions and future lines

Conclusions

Viability of a parallel h+p adaptivity using a non-conformal DDM

Basis functions

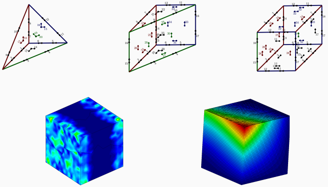

DDM

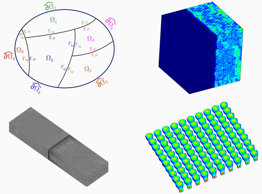

Adaptivity

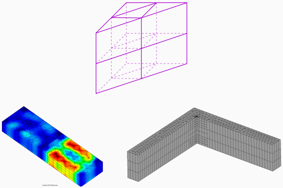

Conclusions and future lines

Future lines

Basis functions:

- Hexahedra in HOFEM with systematic approach.
- Study of the dispersion error.

DDM:

- Introduction of higher order transmission conditions.
- Efficiency in repetitive structures.
- Introduction of a treatment for corner edges.

Adaptivity:

- Introduction of adaptivity with unstructured meshes.
- Support of hanging nodes.
- Application of specific strategies for hp refinement.
- Further study with real structures.

Conclusions and future lines

Contributions

- 3 JCR journals (+ 2 in draft).
- 14 international conferences.
- 2 JCR journals not related to the dissertation.

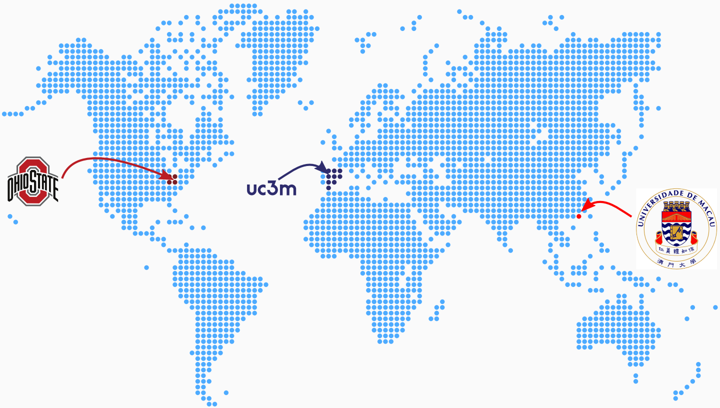
uc3m
UNIVERSIDADE DE MACAU

Thank you!

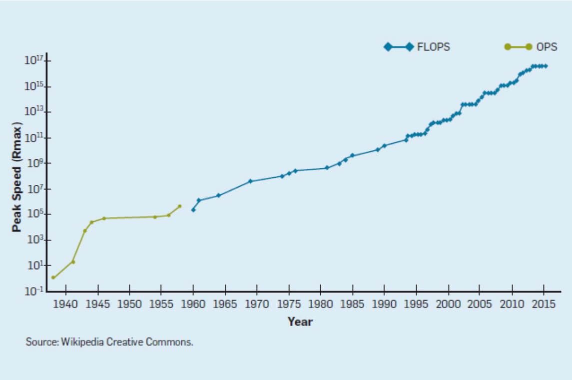
FLOPS
OPS
Peak Speed (Rmax)
10¹⁷
10¹⁵
10¹³
10¹¹
10⁹
10⁷
10⁵
10³
10¹
10⁻¹
1940 1945 1950 1955 1960 1965 1970 1975 1980 1985 1990 1995 2000 2005 2010 2015
Year
Source: Wikipedia Creative Commons.

Mixed order property

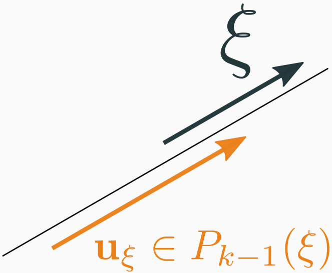

GREMA
RADIOFREQUENCY, ELECTROMAGNETICS, MICROWAVES & ANTENNAS

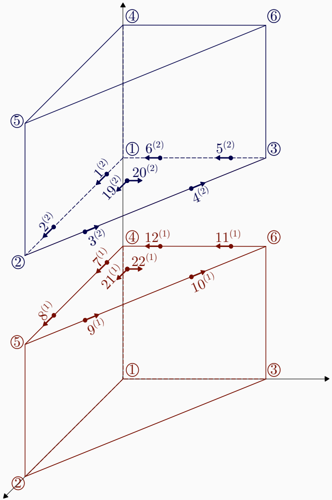

Basis functions: assembling quadrilateral faces

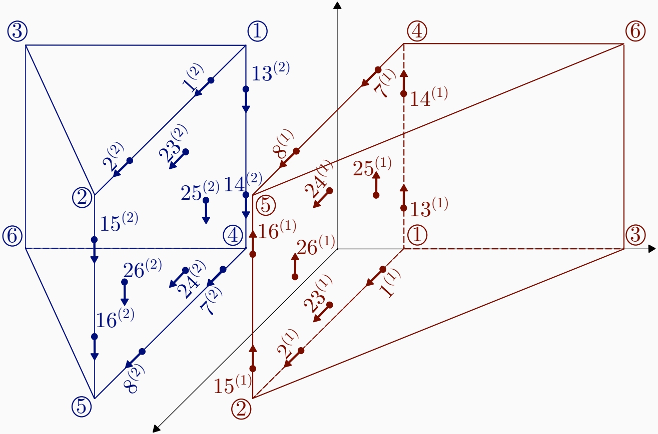

- *vc* version.

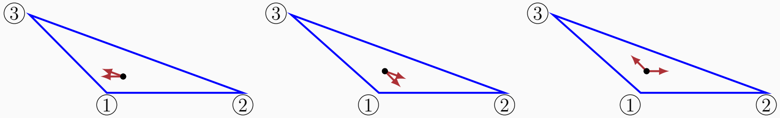

- *vq* version.

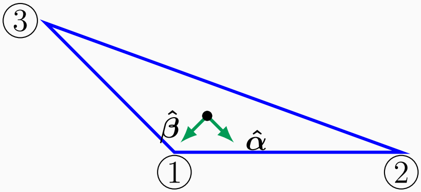

GREMA RADIOFREQUENCY, ELECTROMAGNETICS, MICROWAVES & ANTENNAS

- Condition number: $\frac{|\lambda_{\max}(\mathbf{M})|}{|\lambda_{\min}(\mathbf{M})|}$
- Compared with formulation from other authors: Graglia and Tobon.
  - Interpolatory.
  - Spectral.

$$
\begin{aligned}
L_m L_l^2 \mathbf{W}_{ij};\ & i,j = 1,2,3; j > i; m = i,j; l = 4,5 \\
L_i^2 L_l \boldsymbol{\nabla} L_l;\ & i = 1,2,3; l = 4,5 \\
L_k L_l^2 \mathbf{W}_{ij};\ & i,j,k = 1,2,3; j > i; k \neq i,j; l = 4,5 \\
L_m L_l L_{l+1} \mathbf{W}_{ij};\ & i,j = 1,2,3; j > i; m = i,j; l = 4 \\
L_i L_j L_l \boldsymbol{\nabla} L_l;\ & i,j = 1,2,3; j > i; l = 4,5 \\
L_k L_l L_{l+1} \mathbf{W}_{ij};\ & i,j,k = 1,2,3; j > i; k \neq i,j; l = 4
\end{aligned}
$$

GREMA RADIOFREQUENCY, ELECTROMAGNETICS, MICROWAVES & ANTENNAS

$$[M^p] = [D]^{-1}[M][D]^{-1}$$

$$[K^p] = [D]^{-1}[K][D]^{-1}$$

$$D_{ii} = \sqrt{M_{ii}}$$

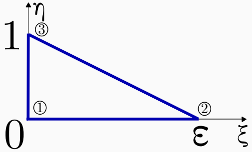

	Reference prism		Triangle deformation					
			$\varepsilon = 4$		$\varepsilon = 8$		$\varepsilon = 16$	
Version	$[M^p]$	$[K^p]$	$[M^p]$	$[K^p]$	$[M^p]$	$[K^p]$	$[M^p]$	$[K^p]$
vc,(1-2)	81	37	1587	210	18826	791	276385	3096
vc,(2-3)	81	37	217	199	738	733	2827	2856
vc,(3-1)	71	38	215	197	737	732	2825	2854
vq	72	37	215	197	737	732	2826	2854
Graglia	37	19	174	104	639	394	2498	1551
Tobon	171	20	842	101	3468	398	14046	1588

GREMA RADIOFREQUENCY, ELECTROMAGNETICS, MICROWAVES & ANTENNAS

$$[M^p] = [D]^{-1}[M][D]^{-1}$$

$$[K^p] = [D]^{-1}[K][D]^{-1}$$

$$D_{ii} = \sqrt{M_{ii}}$$

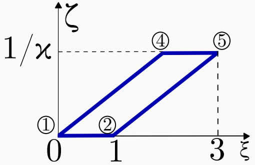

	Reference prism		Rectangle deformation					
			$\kappa = 2$		$\kappa = 4$		$\kappa = 8$	
Version	$[M^p]$	$[K^p]$	$[M^p]$	$[K^p]$	$[M^p]$	$[K^p]$	$[M^p]$	$[K^p]$
vc	72	37	3107	2566	12270	10205	48926	40765
vq	72	37	2187	2066	8435	8171	33432	32599
Graglia	37	19	1484	1067	5889	4279	23509	17131
Tobon	171	20	5967	1209	23559	4226	93928	16923

Results: tetrahedra

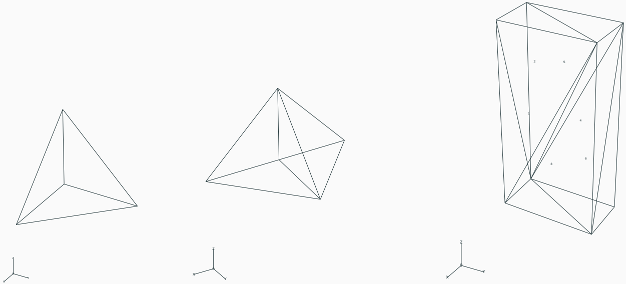

	Parent El.	Example el.2	El. Cube $1 \times 2 \times 4$
vq	128	174	175
vc	138	189	1214

Two face deformation		Four face deformation	
Vertex	Coordinates	Vertex	Coordinates
$\boldsymbol{r}_1$	$(0, 0, 0)$	$\boldsymbol{r}_1$	$(0, 0, 0)$
$\boldsymbol{r}_2$	$(1, 0, 0)$	$\boldsymbol{r}_2$	$(1, 0, 0)$
$\boldsymbol{r}_3$	$(0, 1, 0)$	$\boldsymbol{r}_3$	$(1, 1, 0)$
$\boldsymbol{r}_4$	$(0, 1, 0)$	$\boldsymbol{r}_4$	$(0, 1, 0)$
$\boldsymbol{r}_5$	$(2, 0, 1/\kappa_1)$	$\boldsymbol{r}_5$	$(2, 2, 1/\kappa_2)$
$\boldsymbol{r}_6$	$(3, 0, 1/\kappa_1)$	$\boldsymbol{r}_6$	$(3, 2, 1/\kappa_2)$
$\boldsymbol{r}_7$	$(2, 1, 1/\kappa_1)$	$\boldsymbol{r}_7$	$(3, 3, 1/\kappa_2)$
$\boldsymbol{r}_8$	$(2, 0, 1/\kappa_1)$	$\boldsymbol{r}_8$	$(2, 3, 1/\kappa_2)$

Results: hexahedra (ii)

	Reference hexahedron	Rectangle deformation		
		$\kappa_1 = 2$	$\kappa_1 = 4$	$\kappa_1 = 8$
Version	$[M^p]$	$[M^p]$	$[M^p]$	$[M^p]$
vc	19	912	3552	14112
vq	19	1503	5923	23607

	Reference hexahedron	Rectangle deformation		
		$\kappa_1 = 2$	$\kappa_1 = 4$	$\kappa_1 = 8$
Version	$[K^p]$	$[K^p]$	$[K^p]$	$[K^p]$
vc	30	2131	8721	35168
vq	30	2155	8738	35182

	Reference hexahedron	Rectangle deformation		
		$\kappa_2 = 2$	$\kappa_2 = 4$	$\kappa_2 = 8$
Version	$[M^p]$	$[M^p]$	$[M^p]$	$[M^p]$
vc	19	1869	7405	29552
vq	19	2696	10531	41883

	Reference hexahedron	Rectangle deformation		
		$\kappa_2 = 2$	$\kappa_2 = 4$	$\kappa_2 = 8$
Version	$[K^p]$	$[K^p]$	$[K^p]$	$[K^p]$
vc	30	3689	14616	58318
vq	30	4553	17970	71635

Conclusions and future lines

Dispersion error

- 1992: Lee.
- 1994: Warren, Scott.

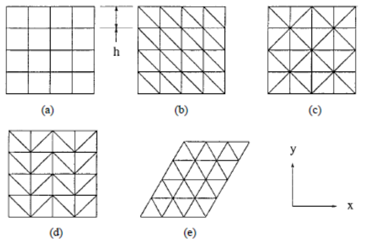

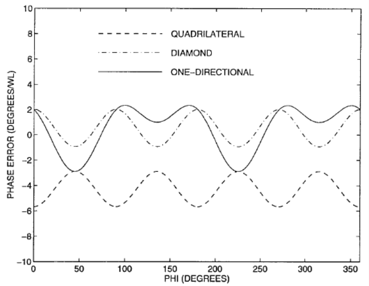

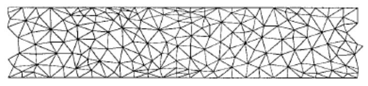

GREMA
RADIOFREQUENCY, ELECTROMAGNETICS, MICROWAVES & ANTENNAS

- 1997: Wu, Lee.
- 2000: Ihlenburg, Babuska: $\mathcal{O}(h^{2p})$.
- 2003: Jin.

- Unstructured triangles in 2D.
- Unstructured tetrahedra in 3D.
- Structured tetrahedra and hexahedra is not encouraged.
- What happens to prisms?
- Tensor product between triangle and segment.

$$\boldsymbol{\mathcal{P}}_{\boldsymbol{k}}^{\text{prism}} = (\mathcal{R}^k(\widehat{T}) \otimes \mathcal{P}_k(\widehat{I})) \times (\mathcal{P}_k(\widehat{T}) \otimes \mathcal{P}_{k-1}(\widehat{I}))$$

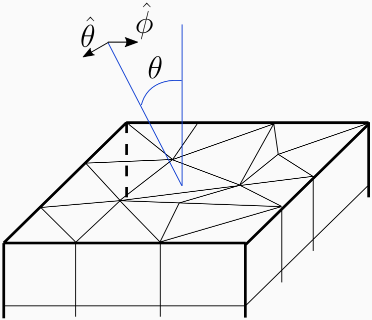

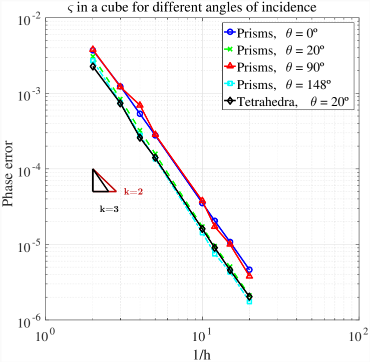

$$\varsigma = \frac{\int_{\Omega} \left| \measuredangle \mathbf{E}^{\theta}_{\mathsf{FEM}} - \measuredangle \mathbf{E}^{\theta}_{\mathsf{MMS}} \right| d\Omega}{\int_{\Omega} \left| \measuredangle \mathbf{E}^{\theta}_{\mathsf{MMS}} \right| d\Omega}$$

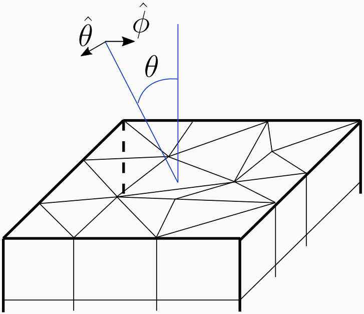

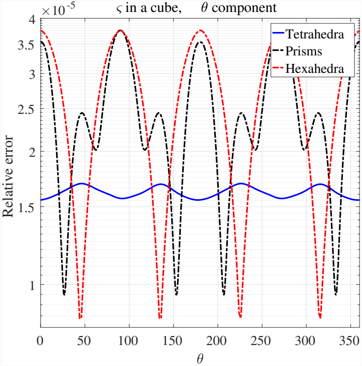

$$\varsigma = \frac{\int_\Omega \left| \measuredangle \mathbf{E}^\theta_{\mathsf{FEM}} - \measuredangle \mathbf{E}^\theta_{\mathsf{MMS}} \right| d\Omega}{\int_\Omega \left| \measuredangle \mathbf{E}^\theta_{\mathsf{MMS}} \right| d\Omega} \tag{2}$$

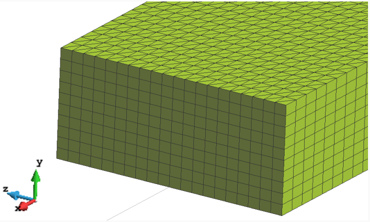

(d) Prism (mesh 1)

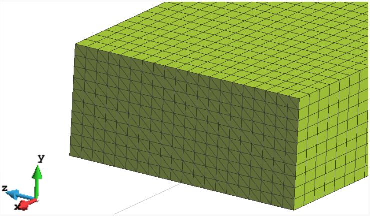

(e) Prism (mesh 2)

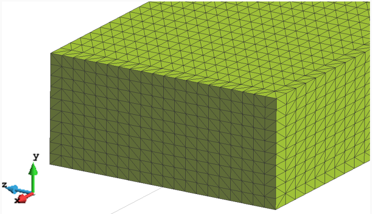

(f) Tetrahedra

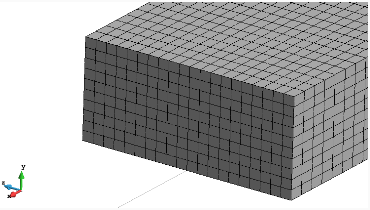

(g) Hexahedra

GREMA
RADIOFREQUENCY, ELECTROMAGNETICS, MICROWAVES & ANTENNAS

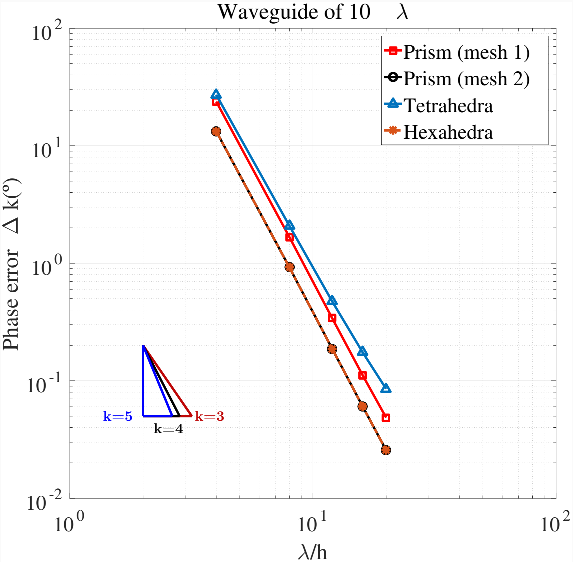

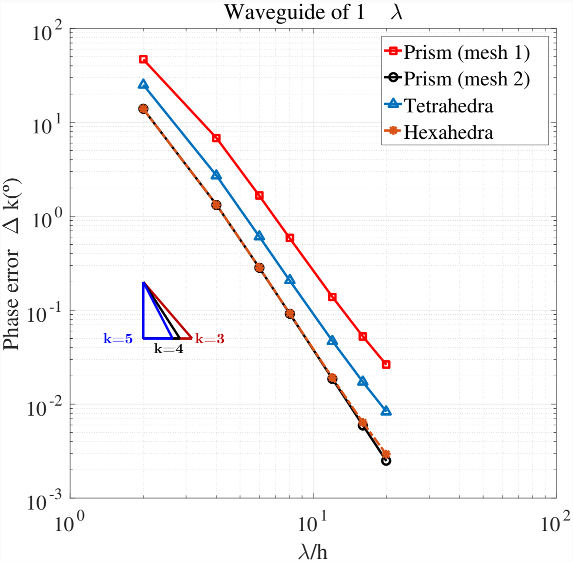
Waveguide of 1 λ
Prism (mesh 1)
Prism (mesh 2)
Tetrahedra
Hexahedra
k=5
k=4
k=3
Phase error Δ k(°)
λ/h
10^2
10^1
10^0
10^-1
10^-2
10^-3
10^0
10^1
10^2

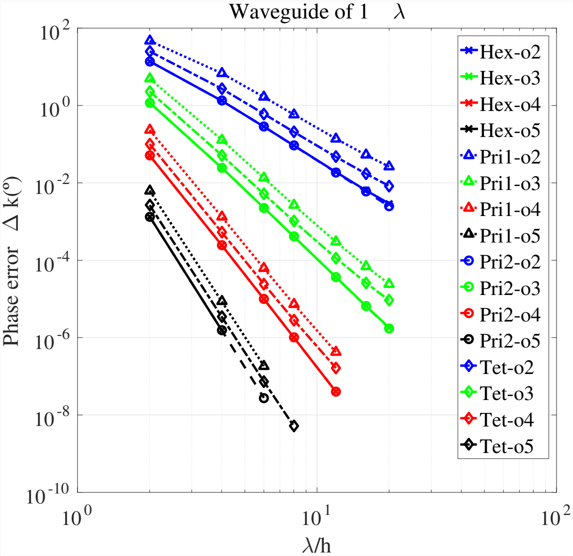
Waveguide of 1 λ
Phase error Δ k(º)
λ/h
10^2
10^0
10^-2
10^-4
10^-6
10^-8
10^-10
10^0
10^1
10^2
Hex-o2
Hex-o3
Hex-o4
Hex-o5
Pri1-o2
Pri1-o3
Pri1-o4
Pri1-o5
Pri2-o2
Pri2-o3
Pri2-o4
Pri2-o5
Tet-o2
Tet-o3
Tet-o4
Tet-o5

Results: waveguide of 1λ (& ii)

	Theory	Experimental value			
Element type	All	Prism 1	Prism 2	Tetrahedra	Hexahedra
Order 2	4	2.917	3.600	3.128	2.895
Order 3	6	5.138	5.883	5.201	5.806
Order 4	8	7.368	7.885	7.419	7.887
Order 5	10	9.498	9.847	9.437	9.764

	Structured mesh	Unstructured mesh
Tetrahedra	9.596e-05	8.414e-05
Prism (mesh 1)	1.461e-03	4.526e-04

GREMA RADIOFREQUENCY, ELECTROMAGNETICS, MICROWAVES & ANTENNAS

$$\varsigma = \frac{\| c_2\left(\left(\mathbf{E}_{\mathsf{FEM}} - \mathbf{E}_{\mathsf{MMS}}\right), \left(\mathbf{E}_{\mathsf{FEM}} - \mathbf{E}_{\mathsf{MMS}}\right)^*\right) \|_2}{\| c_2\left(\mathbf{E}_{\mathsf{MMS}}, \mathbf{E}^*_{\mathsf{MMS}}\right) \|_2}$$

$$c_2(\mathbf{W}, \mathbf{E}) = \iiint_\Omega \mathbf{W} \cdot \varepsilon_r \mathbf{E} \, d\Omega$$

Best approximation error

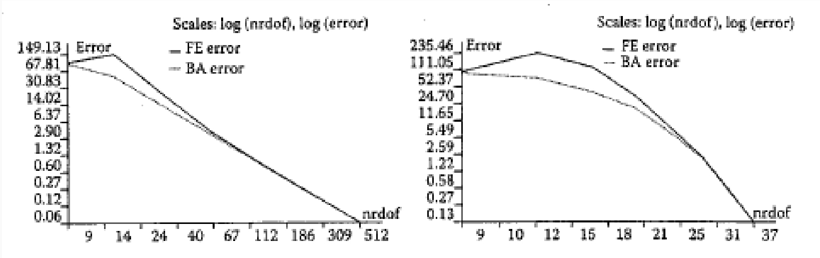

Waveguide error

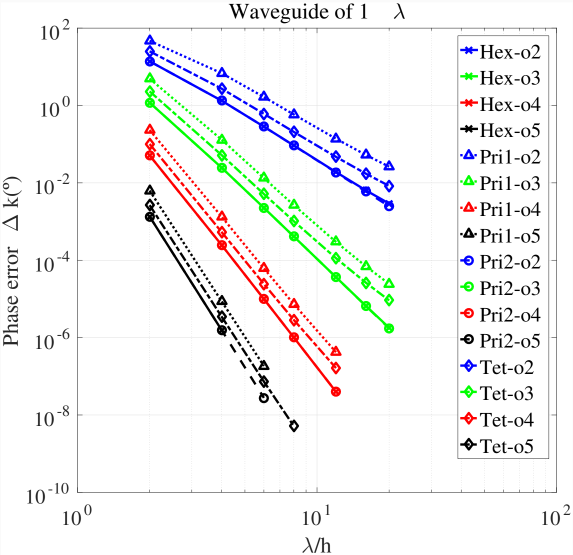

GREMA
RADIOFREQUENCY, ELECTROMAGNETICS, MICROWAVES & ANTENNAS

$$
\begin{aligned}
\alpha =& -jk_0,\\
\beta_i =& \frac{-1}{\Delta_{\mathsf{TE},i} + jk_0},\\
\gamma_i =& \frac{1}{k_0^2 - jk_0\Delta_{\mathsf{TM},i}},\\
\Delta_{\mathsf{TE},i} =& \sqrt{k_{\mathsf{max,TE},i}^2 - k_0^2},\\
\Delta_{\mathsf{TM},i} =& \sqrt{k_{\mathsf{max,TM},i}^2 - k_0^2},\\
k_{\mathsf{max,TE},i} =& C_{\mathsf{TE}}\frac{\pi}{h_{\mathsf{min},i}},\\
k_{\mathsf{max,TM},i} =& C_{\mathsf{TM}}k_{\mathsf{max,TE},i}.
\end{aligned}
\tag{3}
$$

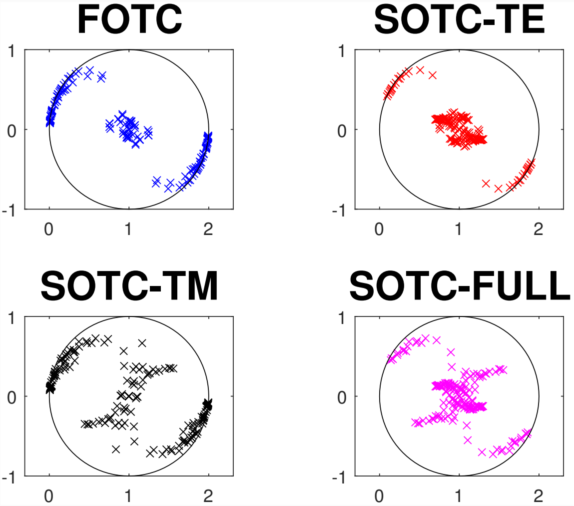
FOTC
SOTC-TE
SOTC-TM
SOTC-FULL
1
0
-1
0
1
2

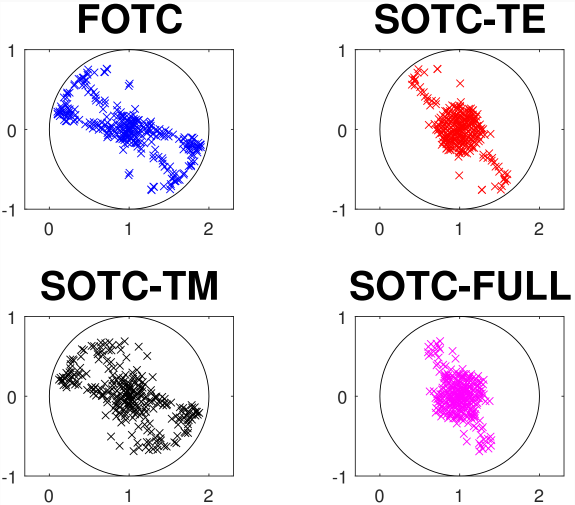
FOTC
SOTC-TE
SOTC-TM
SOTC-FULL
1
0
-1
0
1
2

DDM: comparison with Jin-Fa Lee's group

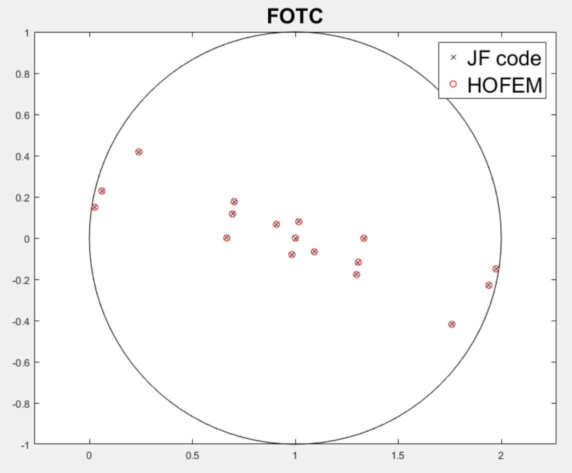

DDM: comparison with Jin-Fa Lee's group

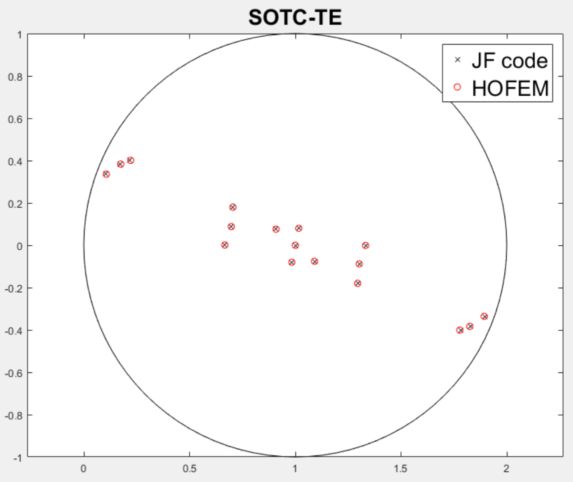

$$|\rho_{TE}| = \left| \frac{jk_z + \alpha + \beta_1 \left(k^2 - k_z^2\right)}{jk_z - \alpha - \beta_2 \left(k^2 - k_z^2\right)} \right|$$

$$|\rho_{TM}| = \left| \frac{j\alpha k_z + k^2 - \gamma_1 k^2 \left(k^2 - k_z^2\right)}{j\alpha k_z + k^2 - \gamma_1 k^2 \left(k^2 - k_z^2\right)} \right|$$

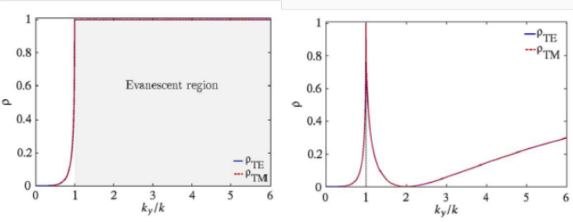

DDM: Corner edge

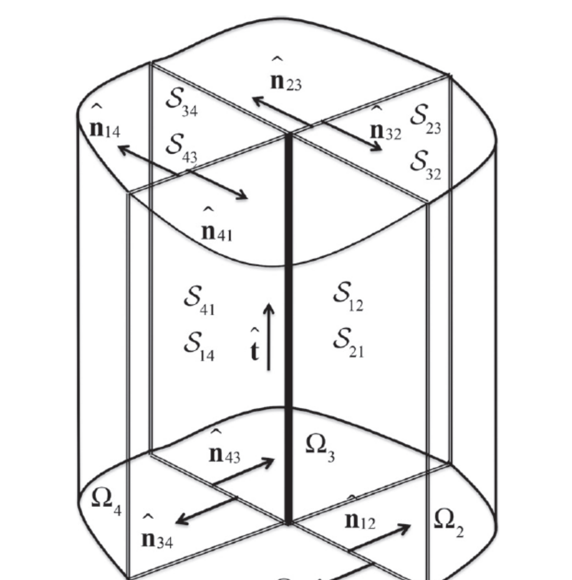

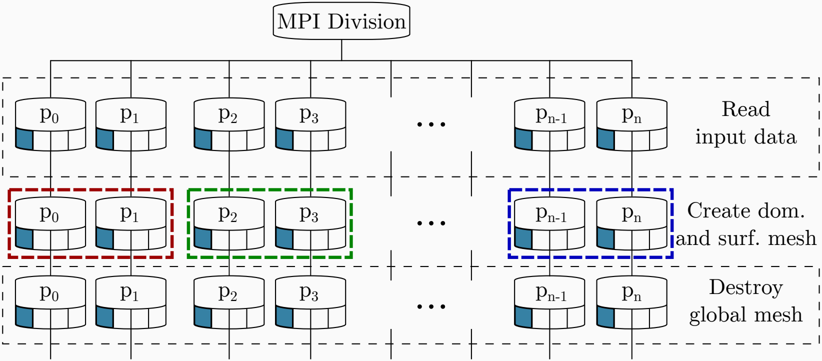
MPI Division
p0
p1
p2
p3
...
pn-1
pn
Read
input data
Create dom.
and surf. mesh
Destroy
global mesh

DDM: workflow (ii)

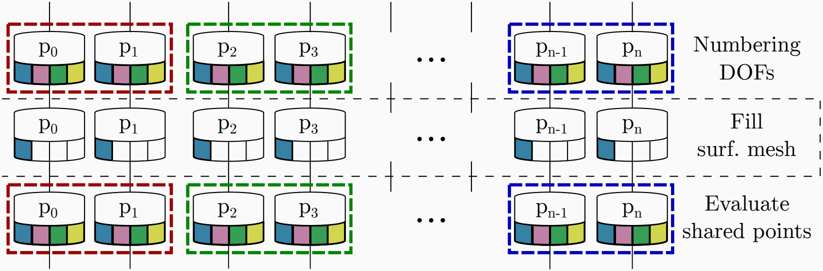

DDM: workflow (iii)

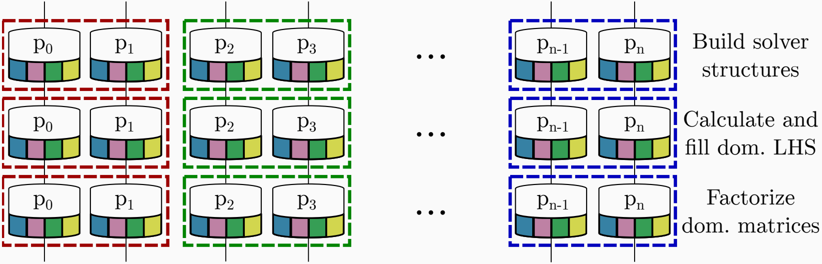

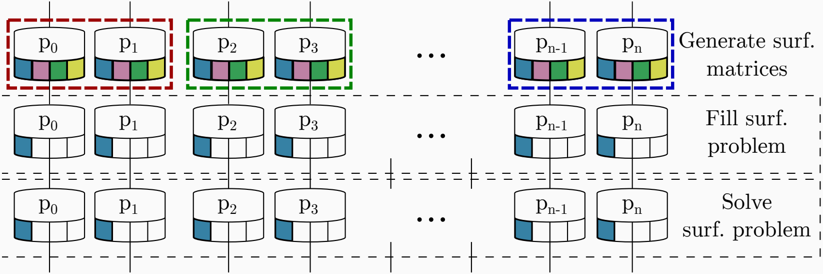

p0
p1
p2
p3
...
pn-1
pn
Generate surf. matrices
Fill surf. problem
Solve surf. problem

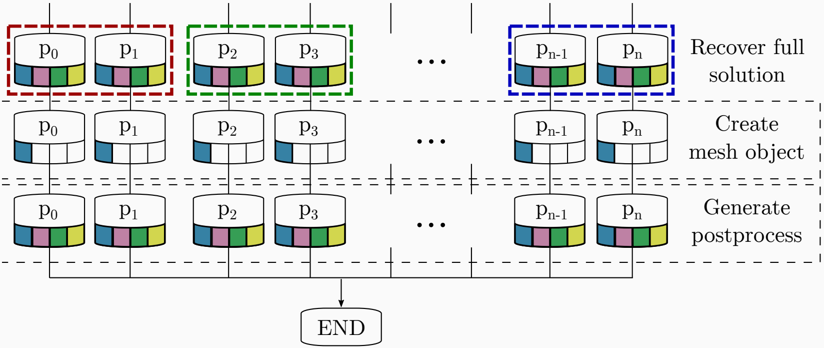
p0
p1
p2
p3
...
pn-1
pn
Recover full solution
Create mesh object
Generate postprocess
END

DDM: different materials

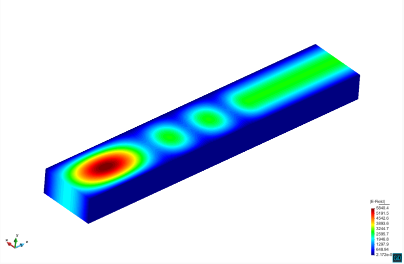

No DDM

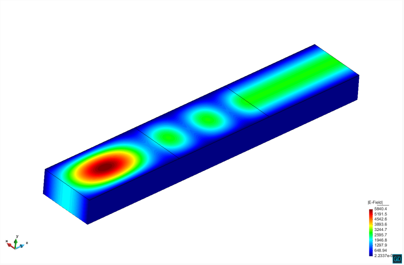

DDM

DDM: filter

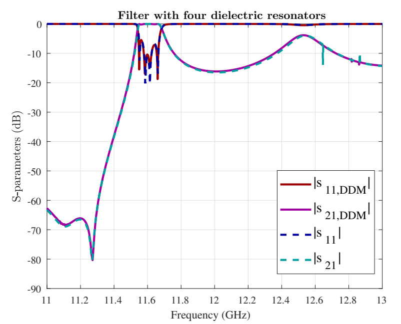

Filter with four dielectric resonators
S-parameters (dB)
Frequency (GHz)
0
-10
-20
-30
-40
-50
-60
-70
-80
-90
11
11.2
11.4
11.6
11.8
12
12.2
12.4
12.6
12.8
13
|s 11,DDM|
|s 21,DDM|
|s 11|
|s 21|

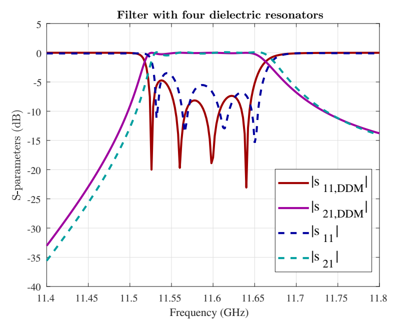

Filter with four dielectric resonators
S-parameters (dB)
Frequency (GHz)
5
0
-5
-10
-15
-20
-25
-30
-35
-40
11.4
11.45
11.5
11.55
11.6
11.65
11.7
11.75
11.8
|s 11,DDM|
|s 21,DDM|
|s 11|
|s 21|

Table 1: Performance results for a two-dimensional antenna array

Case of study	*Time (s)*	*Peak mem.(Mb)*	*Unknowns*
3x3 No DDM	416	5380	1360188
3x3 DDM	463	3371	1398118
4x4 No DDM	1579	12253	2261472
4x4 DDM	1191	5832	2368032

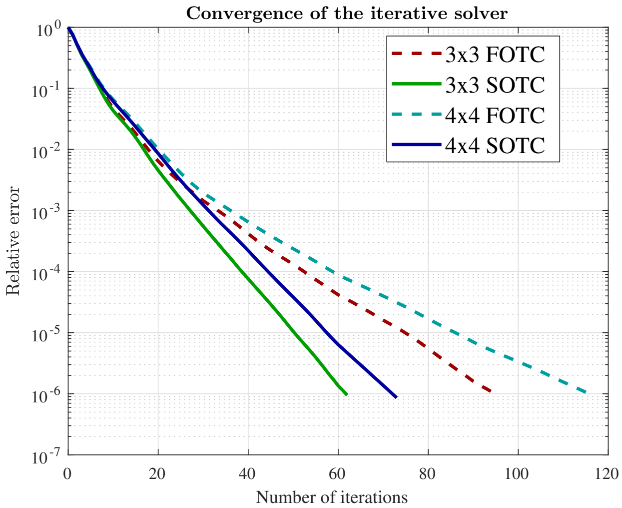
Convergence of the iterative solver
3x3 FOTC
3x3 SOTC
4x4 FOTC
4x4 SOTC
Relative error
Number of iterations
10^0
10^{-1}
10^{-2}
10^{-3}
10^{-4}
10^{-5}
10^{-6}
10^{-7}
0
20
40
60
80
100
120

Performance (iii)

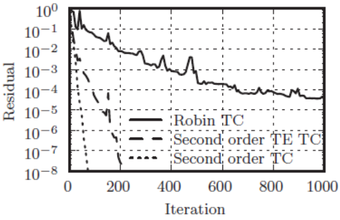

FIG. 4.6. *F-16 iterative solver convergence at* $f = 300$ *MHz.*

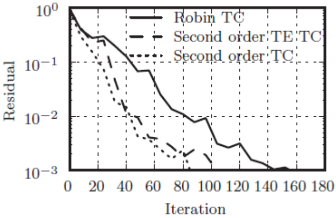

FIG. 4.7. *F-16 iterative solver convergence at* $f = 1$ *GHz.*

Performance (iv)

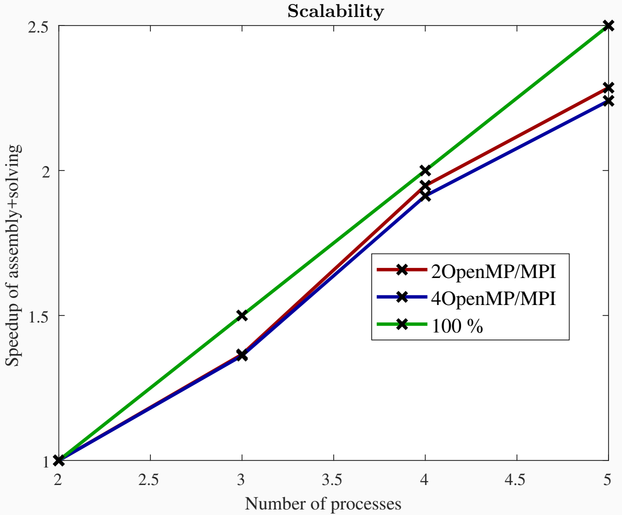

Radiation of circular horn (i)

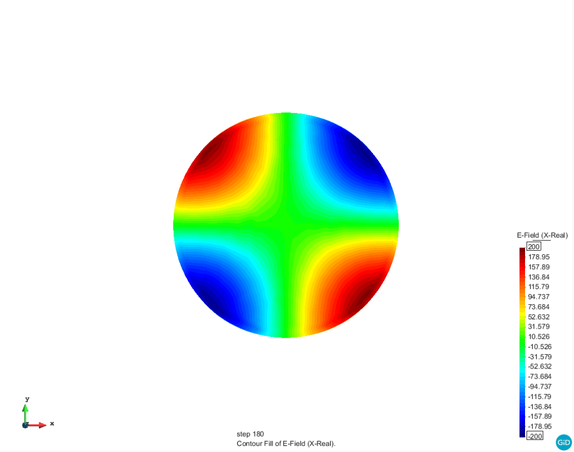

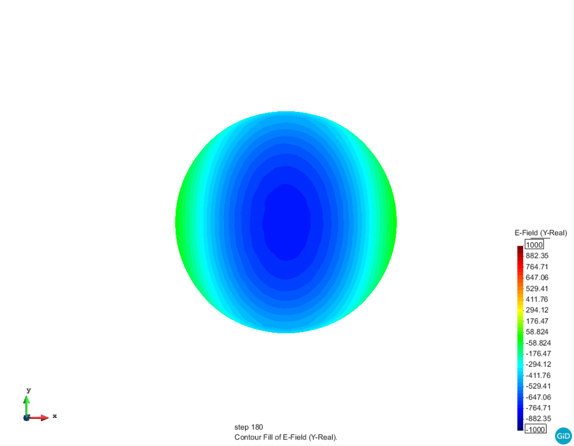
E-Field (Y-Real)
1000
882.35
764.71
647.06
529.41
411.76
294.12
176.47
58.824
-58.824
-176.47
-294.12
-411.76
-529.41
-647.06
-764.71
-882.35
-1000
y
x
step 180
Contour Fill of E-Field (Y-Real).
GiD

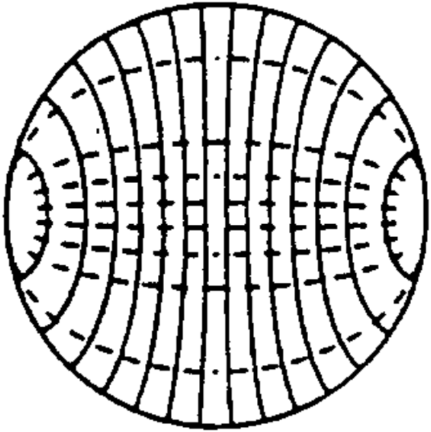

TE_{11}

Radiation of SWA (i)

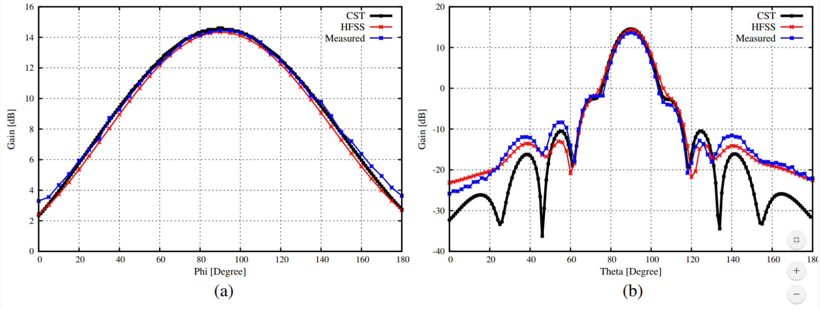

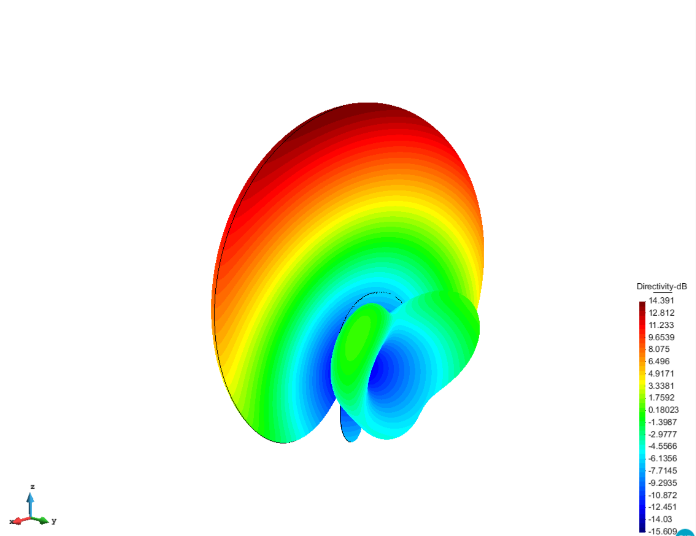

Contour Fill of Directivity-dB.

Estimator for L-shape